



**CHALMERS**  
UNIVERSITY OF TECHNOLOGY

---



# **Quantifying Door Closing Sound Quality**

## **Measurement Techniques and Influence of Selected Parameters**

Master's Thesis in the Master Degree Program Sound and Vibration

**SEBASTIAN SEBALD**



MASTER'S THESIS BOMX02-16-65

# Quantifying Door Closing Sound Quality - Measurement Techniques and Influence of Selected Parameters

SEBASTIAN SEBALD

Department of Civil and Environmental Engineering  
*Division of Applied Acoustics*  
*Vibroacoustics Group*  
CHALMERS UNIVERSITY OF TECHNOLOGY  
Göteborg, Sweden 2016



Quantifying Door Closing Sound Quality - Measurement Techniques and Influence of Selected Parameters

© SEBASTIAN SEBALD, 2016

Master's Thesis BOMX02-16-65

Department of Civil and Environmental Engineering  
Division of Applied Acoustics  
Vibroacoustics Group  
Chalmers University of Technology  
SE-41296 Göteborg  
Sweden

Tel. +46-(0)31 772 1000

Cover:  
Preparation of acoustic camera measurements.

Reproservice / Department of Civil and Environmental Engineering  
Göteborg, Sweden 2016



# Quantifying Door Closing Sound Quality - Measurement Techniques and Influence of Selected Parameters

Master's Thesis in the Master's programme in Sound and Vibration

SEBASTIAN SEBALD

Department of Civil and Environmental Engineering

Division of Applied Acoustics

Vibroacoustics Group

Chalmers University of Technology

## Abstract

Door closing sound is one of the most influential parameters to the customer while buying a car. It is one of the first impressions one can get while interacting with the vehicle and this contributes to the overall quality perception. Thus, it is very interesting for automotive developers to understand the influence of several parameters on the door closing sound quality.

Various experimental and simulation research has already been performed in this field. This thesis is focusing on the experimental part, where classical methodologies, such as standard vibration and acoustical measurements were applied. However, alternative methods, like the acoustic camera, have hardly ever been used. The acoustic camera is typically implemented to measure stationary sound sources. On the other hand, the door closing sound is a transient phenomenon. In this thesis, both, the classical and the acoustic camera approach were used to develop a methodology to quantify the door closing sound quality.

The measurements with the acoustic camera identified various sound sources, distributed over the complete door. The main hot-spots are localized at the striker and around the junction of the upper rail and the B-pillar. The other sources are less contributing to the overall door closing sound. These results have been used to choose adequate measurement positions for accelerometers and were ultimately verified by the classical approach. Based on that, the influence of variations of the door seal stiffness and the inclination of the car were investigated. The main outcome of this was that the door closing sound can be damped or amplified within certain frequency ranges by changing these parameters.

**Keywords:** Door Closing Sound, Acoustic Camera, Stiffness, Hinge Inclination



# Contents

<b>Abstract</b>	<b>i</b>
<b>Contents</b>	<b>iii</b>
<b>Acknowledgements</b>	<b>v</b>
<b>1. Introduction</b>	<b>1</b>
1.1. Background and Purpose . . . . .	1
1.2. Objective . . . . .	2
1.3. Previous Work . . . . .	2
1.4. Scope and Choice of Methods . . . . .	3
1.5. Limitations . . . . .	4
<b>2. Theoretical Background</b>	<b>5</b>
2.1. Door Closing Sound Quality . . . . .	5
2.2. Acoustic Camera . . . . .	6
2.3. Transfer Functions . . . . .	8
2.4. Terminology . . . . .	9
<b>3. Measurement Setups and Equipment</b>	<b>11</b>
3.1. Acoustic Camera . . . . .	11
3.2. Accelerometers & Acoustic Head . . . . .	13
3.3. Boundary Conditions . . . . .	15
3.3.1. Velocity of the Door . . . . .	15
3.3.2. Door Angle . . . . .	16
3.3.3. Measurement Distances . . . . .	16
3.3.4. Frequency Ranges . . . . .	17
3.3.5. Inclination of the Car . . . . .	17
3.3.6. Data Processing . . . . .	17
3.3.7. Background Noise . . . . .	19
3.4. Equipment . . . . .	20

<b>4. Measurement Results</b>	<b>23</b>
4.1. Acoustic Camera . . . . .	23
4.1.1. Reliability of the Camera . . . . .	23
4.1.2. Location of the Sound Sources on the Car Door . . . . .	29
4.2. Classical Approach . . . . .	30
4.2.1. Reliability of the Classical Approach . . . . .	30
4.2.2. Transfer Functions . . . . .	35
4.2.3. Stiffness Variations at Several Positions . . . . .	36
4.2.4. Stiffness Variations at Single Positions . . . . .	39
4.2.5. Varying the Inclination of the Car . . . . .	42
<b>5. Summary and Conclusions</b>	<b>47</b>
<b>6. Outlook</b>	<b>49</b>
<b>References</b>	<b>51</b>
<b>A. Acoustic Camera Measurements</b>	<b>54</b>
A.1. Car 1 . . . . .	55
A.2. Car 2 . . . . .	61
<b>B. Accelerometer and Acoustic Head Measurements</b>	<b>66</b>
B.1. Variation of the Layers . . . . .	66
B.2. Single Stiffness Variations . . . . .	71
B.3. Front Versus Back Inclination . . . . .	76
B.4. Left versus Right Inclination . . . . .	81

# Acknowledgements

I would like to express my deep gratitude to the NVH department at the Volvo Car Corporation, especially to Per-Olof Sturesson and Bo Karlsson, for enabling me the chance to work on this project. I am very grateful to my main supervisor, Ravi Nadampalli, for his great support and high commitment to this research at any time in order to lead this project into the right direction. I also would like to thank Patrik Johansson for the creative input and inspiring discussions, enriching this thesis.

A special thanks to Patrik Höstmad, my examiner and supervisor at Chalmers University of Technology, for his advice, consultation and help during the whole project.

Many thanks to the employees at the Volvo Car Corporation's NVH department, for the interest, the introduction in the very beginning and, especially to Yidan Lai, the continuous supportive input. Also, thanks to the master thesis students assisting me during the acoustic camera measurements.

Finally, I am warmly grateful to my family for the given love, patience, encouragement and strength, enabling me to follow and study my fields of interests, unconditionally of where my journey took me.



# 1. Introduction

## 1.1. Background and Purpose

Within the automotive industry, the door closing sound of a vehicle is of particular interest, since it is one of the most influential parameters to the customer while buying a car. It is one of the first impressions one can get while interacting with the car and this contributes to the overall quality perception. It mainly represents two functions: first, it indicates that the door is properly closed. Second, it contributes an overall impression of the car. Researchers found out that a strong link is existing between the perceived quality and the sound itself [1]. This phenomenon is also not dependent on age, nor on the cultural background of the customer [2]. Thus, it is very interesting for automotive developers to understand the influence of several parameters on the door closing sound quality. The sound quality depends on various parameters of the sound, such as the frequency content, sharpness, loudness, and so on. The sound itself is influenced by parameters like the geometry and material parameters. Depending on these, the sound of the door closing event and thus the quality of the car can be perceived to be pleasant, well closed, annoying, loud, et cetera [2].

Although, various experimental and simulation research has already been performed in this field, many topics have not been investigated. Furthermore, apart from standard approaches, such as measurements with accelerometers and a binaural measurement system, alternative methods, like the acoustic camera, have hardly ever been used. The acoustic camera is typically implemented to measure stationary sound sources. On the other hand, the door closing sound is a transient phenomenon. In this thesis, both, the classical and the acoustic camera measurement techniques were used to enable the quantification of the door closing sound quality. Furthermore, the influence of the door seal stiffness and the vehicle inclination were observed experimentally.

The measurements with the acoustic camera identify various sound sources, distributed over the whole door. The main hot-spots are localized at the Striker and around the junction of the Upper Rail and the B-Pillar. The other sources are less contributing to the overall door closing sound. These results have been used to choose adequate measurement positions for accelerometers and were ultimately verified by the vibration and acoustical measurements. Based on that, the influence of variations of the door

seal stiffness and the inclination of the car were investigated. The main outcome of this was that the door closing sound can be damped or amplified within certain frequency ranges by changing these parameters.

This master thesis has been carried out in cooperation with Volvo Car Corporation. It was of particular interest to implement and test these variations and measurement approaches on the latest vehicle platform, developed by Volvo Cars, the scalable product architecture platform as it is featured in the Volvo S90.

## 1.2. Objective

Classical methodologies to quantify the door closing sound quality are vibration and acoustic measurements, using accelerometers and binaural measurement systems. Another method would be the analysis of the *Operational Deflection Shapes* (ODS), which allows to visualize vibrational patterns on a surface and was part of an earlier thesis, also conducted at Volvo Car Corporation [3]. This methodology is rather laborious and is not necessarily useful to investigate the correlation of vibrations transformed to sound pressure. Another measurement method is the application of an acoustic camera. It is typically used to locate for example leaks within the car body while standing in a wind tunnel. Common source types for this particular type of measurement are stationary sound signals. However, the door closing sound is a very short, impulsive and thus transient sound. Problems might be caused due to that, since acoustic cameras have hardly ever been applied for this type of measurement. Therefore, one task of the of this thesis was to implement this method and validate the results using classical vibration and acoustical measurements. As far as the results of all measurements correspond to each other, the acoustic camera could be a useful tool to locate areas for example on the door surface, which are highly contributing to the perceived sound pressure. These positions would be then interesting for further investigations, by for example mounting accelerometers on them.

Furthermore, the second main objective of this thesis was to investigate the influence of changes of the door seal stiffness and the inclination of the car itself. Both parameters are of particular interest, as they influence the overall door closing sound.

## 1.3. Previous Work

This work is mainly based on the results of *Henrik Törnqvist's and Sofia Wallin's* master thesis "Experimental investigation of mechanisms affecting the door closing sound of passenger cars", conducted at Volvo Car Corporation. In this academic paper, the

authors measured, next to other investigations, the acoustic airborne and vibrational contribution of certain parts of the body of the car, for example of the roof and the hood, during the door closing event. Therefore, accelerometers were mounted on large areas of the car. The results then were analyzed with regards to radiation and via an Operating Deflection Shapes visualization. The airborne contribution was measured by setting up a dummy head with inbuilt microphones in front of the car door. The main outcomes of this thesis was that the radiated sound in lower frequencies was mainly contributed by the doors and dependent on their modal behavior and the force excitation of the striker and the latch [3].

Main purpose of this literature study was to gain experience on current knowledge, both generally and by Volvo, with regards to the topic. Based on that, measurement methods needed to be chosen in order to evaluate the parameters of investigation. The focus hereby was on alternative, new measurement methods. Regarding the door closing sound itself, many studies focused on the psychoacoustic influences, such as the culture, the age, no door seals, loudness, sharpness et cetera [4]. One author discussed several attributes as well as the optimization of the door closing sound itself by analyzing 3D-plots and recommending time values for certain frequency regions [5].

Some authors focused on the creation and verification of computer aided simulations. Examples for that are the simulation of energetic distributions of kinetic energy during the door closing motion[6], the influence of seal stiffness on squeaking and rattling of the vehicle[7].

To draw a conclusion, the papers investigated in this literature study focused mostly on the psychoacoustic or simulation approach. Experimental investigations have not been executed within the specific topics of this thesis. Furthermore, applied measurement methods have not always been mentioned explicitly in most of the experimental papers. This leads to the decision to choose and modify certain measurement techniques of *Törnqvist's and Wallin's* master thesis.

## **1.4. Scope and Choice of Methods**

The main purposes of this thesis were to implement and verify a new measurement method, the acoustic camera, and then, based on the results and experiences, to experimentally investigate the influence of hinge inclination and seal stiffness on the door closing sound. This was done by using accelerometers and an acoustic head. Therefore, the car tested was lifted from several sides to simulate different angles. Also, the stiffness of the door seals was changed at certain positions by compressing it with tape.

To get acquainted with the topic and the measurement systems, a literature study and preliminary measurements were carried out initially.

## **1.5. Limitations**

Like every other measurement as well, this thesis also underlaid certain limitations, influencing the quality and the measurement results. The most important limitation was, that it was not possible to fix all boundary conditions, although most of them were taken care of. One example would be the force input into the door. This was compensated by measuring and keeping the velocity of the door the same.

The frequency range needed to be limited in accordance to the equipment used. The general idea was to measure both, very low and higher frequencies of a certain displacement, using piezoelectric accelerometers. For that, accelerometers of a certain mass were necessary, which ultimately limited the frequency range. Furthermore, it was also necessary to relocate some of the accelerometers to other points of the car, in order to not damage them, for example instead of mounting one directly on the striker. Also, the quality of the results of the acoustic camera depend on various other parameters, such as the distance to the car and the amount of the microphones within the array. This resulted in an even narrower chosen frequency range for this method. Details about the exact frequency range(s) can be found in Chapter 3.3.4.

Also, it was not possible to exchange the door seals completely in order to vary the stiffnesses. This was mainly due to the limited amount of time. Thus, not all initial ideas were realized and tested.

The situations in the laboratories did not represent those in reality. One example would be the varying door closing velocities, depending on the preferences of the customers. Also, the position of the customer next to the car, his or her height, et cetera have significant influences on the perception.

## 2. Theoretical Background

This chapter presents the theoretical background about the basic principles of this thesis. Only a brief overview is given for most of the chapters. However, for more detailed information about a certain topic it is recommended to look at the references.

### 2.1. Door Closing Sound Quality

Door closing sound quality can be described subjectively and depends on the impressions and preferences of the listener. Thus, the automobile industry performed various studies in order to define “good” and “poor” sound quality. It is a complex sound, depending on many parameters, such as loudness, sharpness, existence of rattles, frequency content, et cetera. *Hamilton* studied these influences and set up the following conclusions, defining an ideal door closing sound: the closing event should not generate “unexpected” sounds, such as squeaking and rattling. If that is not the case, the customer might perceive the car to be of less quality. The sound should be dominated by lower frequencies, the content of higher frequencies needs to be minimized. A lower frequent sound is usually associated to a big mass and thus can be connected to a solid source.

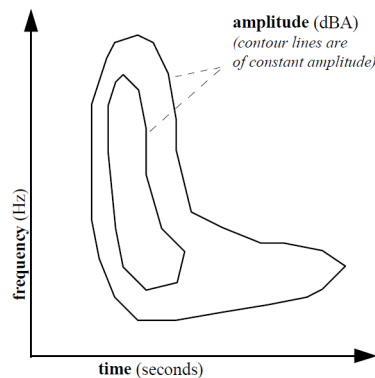


Figure 2.1.: Ideal “sound figure” for a door closing event. (Hamilton, 1999)

Optimal lengths of sounds with respect to time should be 0.150 s for the initial impact, and 0.5 s to 0.6 s for the whole event, where 0.4 s to 0.5 s should be dominated by lower

frequencies. *Hamilton* summed up his investigations and created a “sound figure”, as presented in Figure 2.1, defining an optimal time-frequency-shape of the event [5].

## 2.2. Acoustic Camera

One of the main goals of this thesis is to implement and test the usability of a new measurement method, the acoustic camera. Using an array of for example 30 microphones, it allows to visualize and localize sound sources within the field of view of the camera. Receiving a signal of a sound source, it is perceived differently by each microphone of the array, depending on the distance between the source and the microphone. Typical methods for the near-field are for example acoustic holography and beamforming for the far-field. Furthermore, inverse methods are also existing. For this thesis, only beamforming is of interest, as the camera needs to be placed at a certain distance to the door in order to assure a proper door closing movement. This automatically excludes near-field measurements, since the camera therefore needs to be placed very close to the door, depending on the frequency range of interest [8].

When applying beamforming, the signals received by each microphone are relatively delayed and then summed up. Thus, a time signal is calculated, which then can be assigned to its' individual source. The advantage of this method is the cancellation of noise, caused by other sources since only signals from a certain source are amplified due to the time correction. Those coming from other sources can interfere negatively with each other [9]. This is especially useful for a typical application of beamforming: within a wind tunnel to locate for example leaks in the structure of the car with a high background noise caused by the wind. This and other usual applications, like testing the door seal for leaks by using a white noise source inside a car, however are generally stationary sound sources. Since this thesis is dealing with a transient, impulsive signal, it is questionable, whether the acoustic camera can also be used for this type of application since the signals are rather short. This could cause problems for example in the post-processing of the measurement data. In order to gain knowledge of the structural and vibrational behavior of the door during the closing event, the first impact of the door on the frame is of particular interest, since it symbolizes the main and thus primary source of sound at a position to be determined. Thus, this work focused on the first impact only for the acoustic camera measurements.

### *Frequency Range Limitations:*

The frequency range of the acoustic camera, while applying the beamforming method, is determined by two different factors. The lower limit can be estimated by calculating the spacial resolution  $R$  [10], a measure of how distinguishable two sources are, as it

can be seen in Equation 2.1:

$$R = \frac{L}{D} \lambda \text{ in } m \quad (2.1)$$

Here,  $L$  represents the distance to the source,  $D$  the diameter of the array and  $\lambda$  the wavelength. A high value for  $R$  describes a low spatial resolution, which means that for example two sources close to each other can not be distinguished from each other. This can be the case for too low frequencies. A low value of  $R$  stands for a high spatial resolution on the other hand, for example for high frequencies. Then, both sources can be recognized independently.

The upper frequency limit is mainly determined by two different factors, the distance between the microphones of an array with linear distribution, or by the dynamic range for an array distributing the microphones randomly. For this thesis, only the dynamic range is of importance since an array with randomly distributed microphones was used. The dynamic range is basically the level difference  $\Delta L$  of the main lobe and the side lobe. The main lobe represents the direction of radiation with the highest acoustical power, whereas the side lobes describe lower radiation in other, undesired directions. Figure 2.2 illustrates this topic perfectly. With increasing frequencies, the level difference of the described lobes decreases, which causes results of lower quality. The dynamic range is influenced by the number of microphones used during the measurements. Even minor changes can result in a significant decrease of the upper frequency limit.

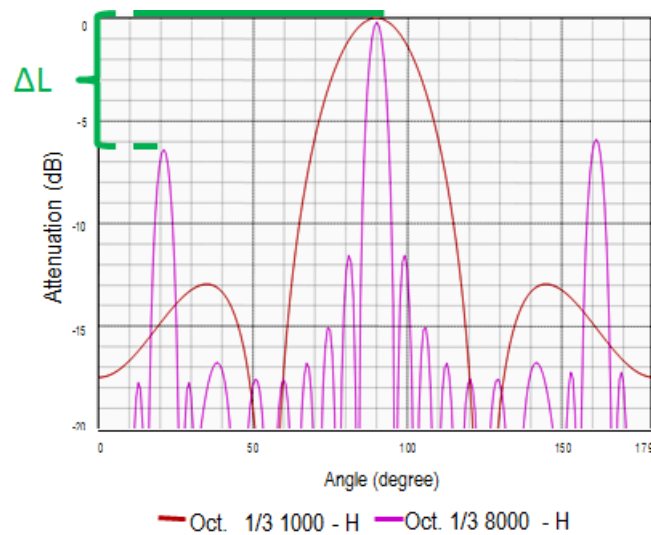


Figure 2.2.: Main lobe and side lobes of a radiated signal. (LMS)

## 2.3. Transfer Functions

The relation between two signals can be described using two different measures: coherence and frequency response function.

Generally, the frequency response function is the relation of the output signal  $Y(f)$  to the input level  $X(f)$ , both in the frequency domain, as it can be seen in Formula 2.2. A typical example for this type of calculation would be the correlation between two points of a structure while exciting one with an impact hammer and measuring the frequency response at another by using an accelerometer.

$$H(f) = \frac{Y(f)}{X(f)} \quad (2.2)$$

For measurements like this, using a single input and a single output, Formula 2.2 can be transformed to  $H_1(f)$  and  $H_2(f)$  as seen in Formula 2.3. There,  $S_{xx}(f)$  and  $S_{yy}(f)$  represent the auto spectral density in the frequency domain of  $X(t)$  and  $Y(t)$ .  $S_{xy}(f)$  stands for the cross spectral density of the input and the output signal and  $S_{yx}(f)$  for that of the output and the input signal. Both are also located in the frequency domain of  $X(f)$  and  $Y(f)$ . Depending on the noise within the measurement signals,  $H_1(f)$  should be chosen if low noise is expected at the input signal,  $H_2(f)$  on the other hand if low noise is expected for the output signal.

$$H_1(f) = \frac{S_{xy}(f)}{S_{xx}(f)} \quad \text{and} \quad H_2(f) = \frac{S_{yy}(f)}{S_{yx}(f)} \quad (2.3)$$

In case of an ideal coherence,  $H_1(f)$  and  $H_2(f)$  will show the same results [11].

Thus, and as a second method, the coherence is an important tool and alternative to evaluate the correlation of two signals. It is technically the degree of consistent linear dependency of two signals of two single channels in the frequency domain and can be calculated as shown in Equation 2.4.

$$y^2 = \frac{H_1(f)}{H_2(f)} = \frac{|S_{xy}(f)|^2}{S_{xx}(f) \cdot S_{yy}(f)} \quad (2.4)$$

A coherence equal to 1 represents a very good correlation of the input level to the output level, whereas a low value stands for the opposite. Then, the signal can be influenced by noise and other uncertainties. In order to achieve a good coherence, it is also necessary to average over several measurements. A usual number would be 10 - 20 measurements [12].

## 2.4. Terminology

Within this thesis, a certain terminology needed to be established for the different measurement positions and areas on the front door of the car. Basically, the traditional technical terms were used and enhanced by adding specific names of location. The terminology applied can be found in Figure 2.3.

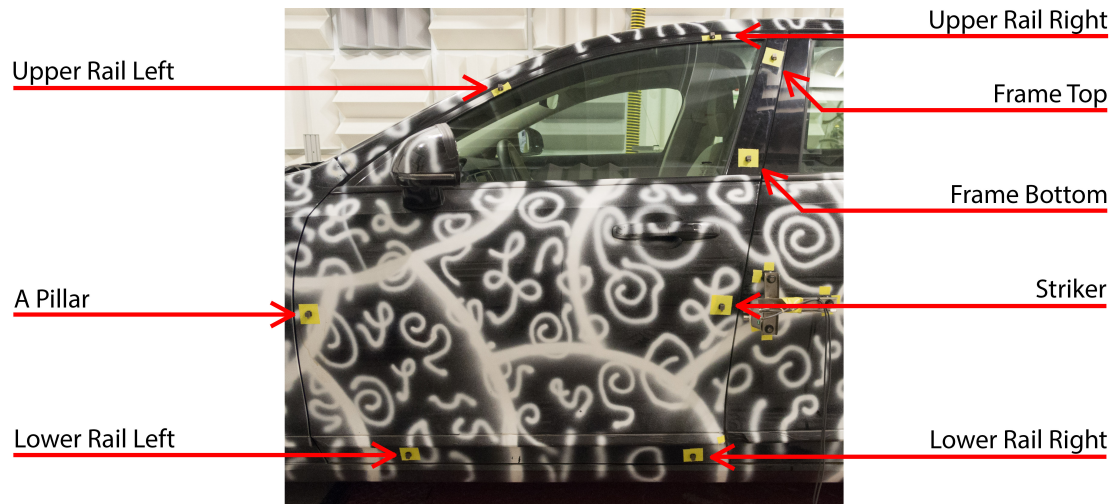


Figure 2.3.: Terminology used for different areas of the front door.

Additionally, for the analysis of the acoustic camera, the term “hot-spots” was implemented and describes the areas of the car, where the acoustic camera measured higher sound pressure levels than in comparison with the surrounding area and thus are sources of relatively stronger sound radiation. An example for a hot spot can be found in Figure 2.4.

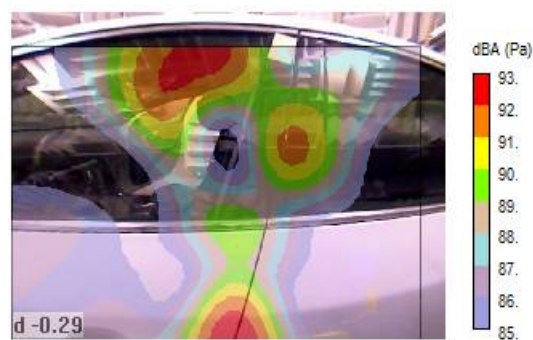


Figure 2.4.: Examples for “hot-spots” on the car.



## 3. Measurement Setups and Equipment

All measurement setups and procedures applied are being described in detail in this chapter, as well as the equipment used. The following measurements have been carried out:

*Acoustic Camera:*

- Basic measurements
- Validation measurements

*Classical Approach:*

- Basic measurements
- Changing the stiffness of the door seal at certain positions
- Changing the angle of the car

### 3.1. Acoustic Camera

The first type of measurements carried out was the approach using a high definition acoustic camera, produced by *Siemens/LMS* [14]. The idea was to capture all appearing sources on the front door of the car. The setup was relatively simple and can be seen in Figure 3.1. There, the acoustic camera was placed at a certain fixed distance in front of the door. The device then was connected to a *LMS* front-end, which was plugged into a measurement computer with *LMS.Testlab* software. Furthermore, the camera itself was also connected to the computer directly. Due to difficulties with the equipment, only 28 out of 36 microphones were used of the array. This however was still ensuring sufficiently enough data for calculations. On the other hand, certain limitations due to this choice of the setup were expected, introduced by the missing microphones.

Since the camera cannot cover the whole door at once, due to a decrease of measurement quality depending on the distance to the source, it had to be moved to several different measurement positions while investigating the same setup of the door in order to get good quality results. For measurement positions close to the floor, several

layers of porous absorbers needed to be placed on the floor in order to avoid reflections that can influence the results of the camera.



Figure 3.1.: Measurement setup using an acoustic camera.

Several measurements have been carried out with the acoustic camera. The measurements of the original setup of one vehicle without any modifications were the main measurements, in order to achieve the most interesting hot-spots for later accelerometer measurements. For the validation of the measurements, another measurement row has been carried out on another car, applying the same setup. The average length of a measurement was 2 s.

All in all, three measurements within a certain door velocity range, which will be further explained in Chapter 3.3.1, have been taken per camera position. Also, in order to not move the camera during these measurements, the door needed to be closed from inside the car.

*Expected Results:*

Based on the general knowledge and the results of the literature study, the main expected source to be seen is located at the striker. Other sources should be located along the B Pillar of the car. However, the region close to the A Pillar should have less influence on the door closing sound.

## 3.2. Accelerometers & Acoustic Head

The second type of measurements was conducted by applying accelerometers and an acoustic head in order to measure acoustical and vibrational levels on the door. Eight accelerometers have been mounted on top of the outer surface of the front door as it is shown in Chapter 2.4, Figure 2.3. The accelerometers have been directly placed on the yellow interlayer of tape by applying special clips. Thus, the car was not damaged by the measurements. The positions have been chosen in accordance to the acoustic camera measurements (which will be described more thoroughly later) and in order to validate the results of those. It was assumed that all parts used, namely clips, glue and tape, did not influence the measurements significantly, and that the accelerometers were mounted rigidly on the surface. All accelerometers then were connected to a front-end, an *OctoBox+* by *Head Acoustics*, which was connected to the measurement computer.



Figure 3.2.: Measurement setup using accelerometers and an artificial head microphone.

The acoustic head, produced by *Head Acoustics*, was placed in front of the car door handle. It was directly connected to the front-end and thus also to the computer. The complete measurement setup can be seen in Figure 3.2.

The following measurements have been carried out: at first, the sound pressure and acceleration levels of the basic setup without any changes have been measured. Then, the stiffness of the door seals have been modified. In the first variation, one layer of tape has been mounted on the seal next to the striker, the frame bottom and the upper rail right, see Figure 3.3, increasing the stiffness locally. For the second variation, an additional layer of tape has been attached to the same positions. Last but not least, each one of these spots have been tested individually on their influence on the door closing sound by only putting one layer of tape to those, separately. An example can be seen in Figure 3.4



Figure 3.3.: Stiffness variations at three different positions.

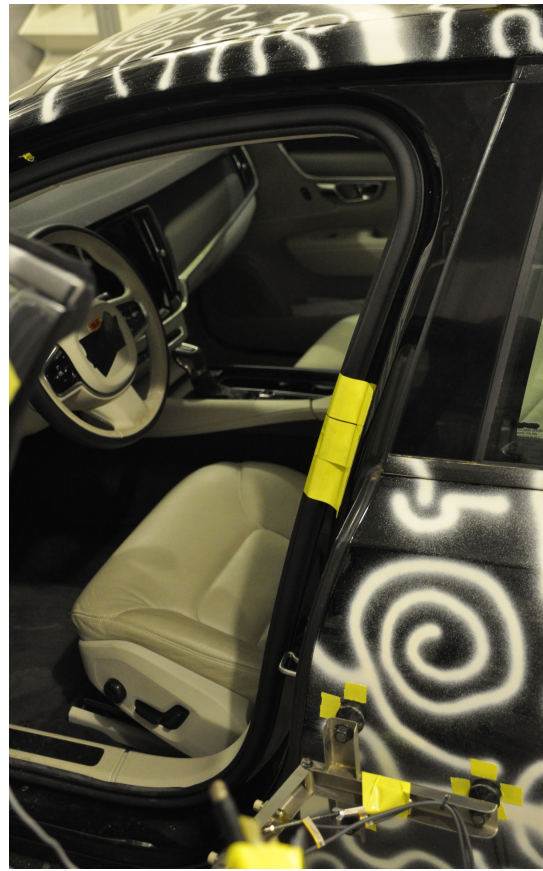


Figure 3.4.: Stiffness variation at one particular position.

The software in use was *Head Recorder*. All accelerometers were calibrated manually using a hand-held calibrator. The microphones of the acoustic head were pre-calibrated.

Overall, three measurements have been taken for each variation assuring a sufficient amount of data to compare with.

### 3.3. Boundary Conditions

One of the main tasks of this thesis was to ensure repeatability and to avoid as many uncertainties as possible. Those uncertainties can be caused by for example environmental influences, measurement uncertainties, electric noise in the cables, et cetera. Therefore, these influences need to be reduced to a minimum by setting boundary conditions which are presented within the following sub-chapters.

#### 3.3.1. Velocity of the Door

The velocity of the door during the closing event is the most important boundary condition to fix. Variations of the velocity during different measurement setups of the door can influence the final results significantly and will thus reduce comparability. These discrepancies are caused by varying forces implemented in order to close the door by hand. A higher force input means a higher door velocity. Preliminary measurements showed that a variation of  $\pm 0.05$  m/s can have significant influence on the data acquired. However, a variation of  $\pm 0.03$  m/s is still acceptable as the results are comparable enough, which will be also shown in Chapter 4.2.1.

The nominal velocity was chosen and set to a value of 1.00 m/s, which was shown to be the natural closing velocity in accordance to *Törnqvist's & Wallin's* previous work [3].

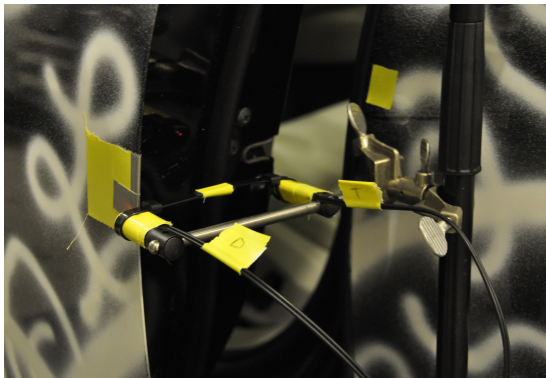


Figure 3.5.: Free standing velocity sensor for the measurements using the acoustic camera.



Figure 3.6.: Magnetic velocity sensor applied during the classical approach.

To measure the velocity, two custom built door velocity sensors have been used during

the measurements as shown in Pictures 3.5 and 3.6. One was directly mounted on the rear door via magnets (Figure 3.5, for the measurements using accelerometers), and the other one, for the acoustic camera measurements, was standing very close to the door, see Figure 3.6. In both cases, the positions were fixed and care was taken so that both had no influence on the closing sound.

All measurements used for analysis in this thesis have been carried out within the accepted range of velocity, as described above.

### **3.3.2. Door Angle**

Another boundary condition to fix was the initial opening angle of the door. It is of particular importance in order to assure a constant acceleration of the door during the closing event. A wider angle in comparison with other measurements could cause a significantly lower door closing velocity shortly before the impact and thus a lower force of the door itself when hitting the frame and the striker. Therefore, the initial angle of the door needed to be set. Thus, for the vibration and acoustical measurements, the door was always opened until the first check-link, the first point where the door locks itself slightly into position. The door then had an angle of  $35^\circ$ .

### **3.3.3. Measurement Distances**

The distances of some of the measurement equipment was also one important boundary that needed to be fixed. For the acoustic head, it was placed in front of the front door handle with a distance of 1.00 m and a height of 1.70 m. This is again in accordance to *Törnqvist's & Wallin's* thesis [3].

The distance of the acoustic camera to the door was generally set to 0.50 m. It was the minimum space in between the door and the camera in order to perform beamforming measurements, set by the recommendation of the supplier [13]. It was necessary to place the camera closer to the car since the spatial resolution and thus the quality of the results are depending on the distance. The further the camera is away, the worse the results will be and the higher the lower frequency limit will be. The distance was measured automatically by the camera itself. However, since the distance sensor did not always measure the correct distance during the measurements with the first car, due to reflections or the glass surface, it was measured manually as well and corrected later within the software. It was also necessary to slightly adjust the angle of the camera in order to be always parallel to the surface of the car.

### 3.3.4. Frequency Ranges

The frequency ranges for the measurements also needed to be chosen. Depending on the measurement methods, different frequency ranges of interest have been set:

#### *Acoustic Camera:*

When using the acoustic camera, the frequency range is limited by several factors. The minimum frequency determines the quality of the result (by the spacial resolution) and is influenced by the distance of the camera to the object of interest, as described in Chapter 2.2. In accordance to the suggestions of the supplier of the camera, the lowest frequency for achieving good results in this case is 600 Hz, where a  $R$ -value of about 0.55 m can be expected, which basically is a rather low spatial resolution. The upper frequency range is also limited due to the dynamic range. According to the supplier, the upper frequency limit is specified with 20000 Hz for 54 microphones [14]. For an array with originally 36 microphones, as used in this case, the upper frequency limit has been manually calculated and was finally set to 10000 Hz. However, since fewer microphones were used, it is expected, that side lobes can be already visible at lower frequencies.

#### *Classical Approach:*

As described in Chapter 2.1, the main frequencies of interest are within a range of 10 to 4000 Hz. Therefore, this range has been selected and suitable measurement equipment has been chosen accordingly.

### 3.3.5. Inclination of the Car

For the measurement of the influences of door inclination on the door closing sound, the car needed to be angled. This was done by applying two lifters, lifting up one side of the car, and by mounting a digital protractor on top of the roof of the car as shown in Figure 3.7

The vehicle was lifted from the front, back, left and right, applying angles of  $0.5^\circ$  and  $1.0^\circ$ .

### 3.3.6. Data Processing

In order to compare the measurements, the signals needed to be cut and processed equally within the same method. For the two measurement approaches, the following techniques of signal processing have been decided:

#### *Acoustic Camera:*

The sound pressure levels of the highest amplitude are expected to be radiated by the



Figure 3.7.: Measurement setup while angling the car.

source during the closing event. The localization of the source with respect to secondary and after impacts cannot be detected by the camera since it highlights the position where sound is radiated or where sound waves are traveling. By the time of the secondary impacts, the sound radiation is highlighted at another position as the sound waves already passed the exact source earlier. Taking this into consideration, only the initial impact is of particular interest to identify the dominant radiating sound sources. Thus, a time window of the length of roughly the first impact was chosen, in order to only analyze this impact. It was decided to always use a time window of the length of 0.053 s. To achieve such a short interval, a frequency resolution of 40 Hz had to be chosen. An example for the different impacts and the chosen signal length, marked with the green lines, can be seen in Figure 3.8.

Due to time limitations it was also decided to analyze the results in steps of  $3^{rd}$ -octave bands. The program then averaged the measured results within each band. It is expected that this might cause some limitations, however, this step was compulsory in order to show meaningful results in a reasonable time frame.

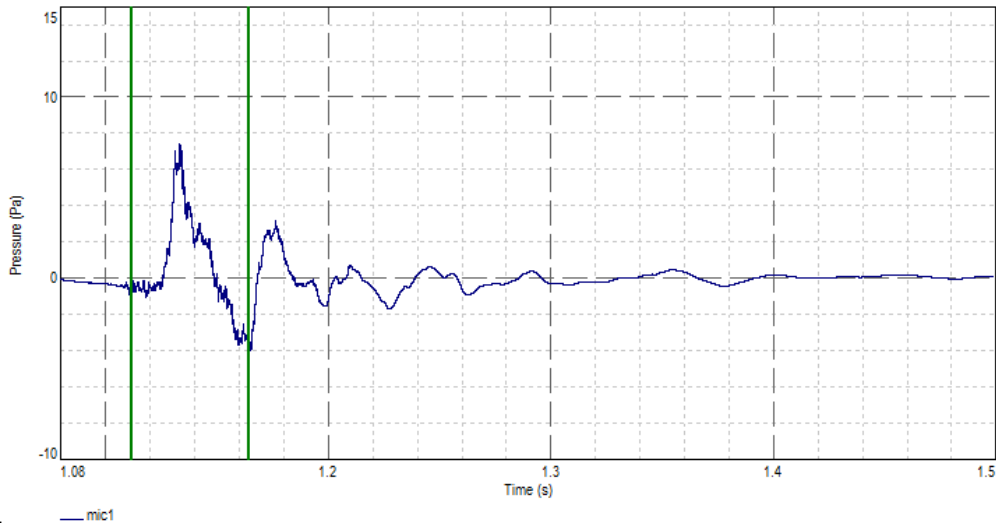


Figure 3.8.: Typical measured impulse response with a chosen time window, unweighted.

*Classical Approach:*

For the accelerometers and the acoustic head it was decided to use a time window of roughly the length of the whole impulse in order to capture all vibrations caused due to the impact and to avoid too much irrelevant noise. Therefore, the window length was set to 0.805 s as shown in Figure 3.9. The results then were transformed from narrow-bands to 3<sup>rd</sup>-octave bands.

*General:*

For calculations, such as the fast-fourier-transformation or coherences, a window function has to be applied. The best solution for impulsive signals is commonly no window or an exponential window. Since both are not applicable in the software used, a rectangular window function has been chosen.

All sound pressure levels were A-weighted.

### 3.3.7. Background Noise

The background noise needs to stay sufficiently low in order to assure measurement results of high quality. Therefore, the background noise level has been measured before every measurement row and was always low enough, thus, the measured signals were not influenced by it.

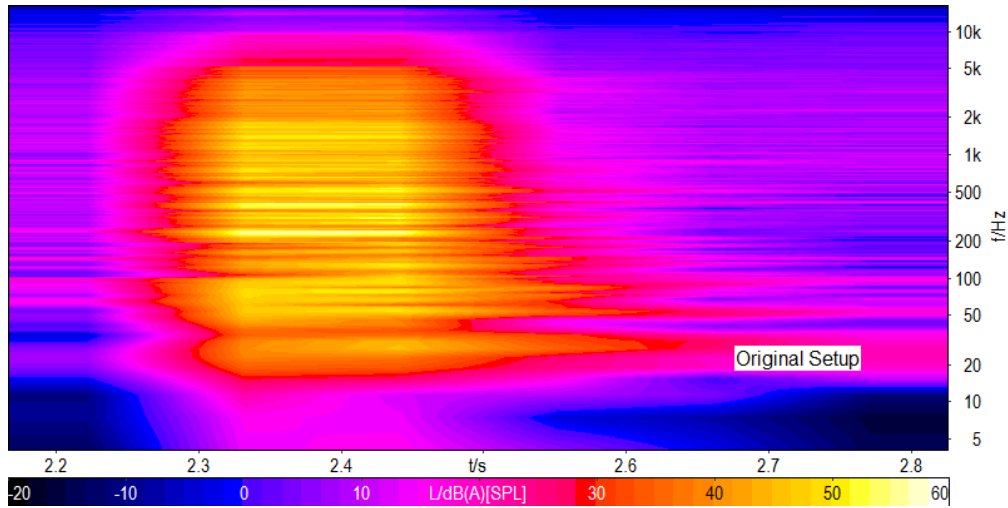


Figure 3.9.: Typical measured impulse response with the length of the chosen time window, A-weighted.

### 3.4. Equipment

The following equipment has been used for the measurement using the acoustic camera:

Name	Company	Type	Serial Number	Notes
High Definition Acoustic Camera	Siemens/LMS	GLI	1226:01:00	
Front-end	Siemens/LMS	SCM05	53131001	
Optical Sensors	Keyence Corp.	RV-1213:1	2558772	used to build a custom door velocity sensor
		RV-1212:1	2567986	
Timer/Counter 120 MHz	Philips	PM6665	92430-UTL-PV14	
Digital Protractor	Mitutoyo	Serie 950 - Pro 360	15100348	
Force Gauge 1 kN	Mark-10	M5-200	3461570	to not damage the car, a steel interlayer has been applied

Table 3.1.: Equipment used during the acoustic camera measurements.

For the sound pressure level and vibrational measurements, the following equipment has been applied:

Name	Company	Type	Serial Number	Notes
Front-end	Head Acoustics	OctoBox+	33110150	
Binaural Measurement System	Head Acoustics	HDM I.O	13000042	
DeltaTron Accelerometers	Brüel & Kjær	Type 4507	2203562	Ch. 8: A Pillar
			2203559	Ch. 7: Lower Rail Left
			2203558	Ch. 6: Lower Rail Right
			2203552	Ch. 5: Upper Rail Left
		Type 4507 B	2307547	Ch. 4: Upper Rail Right
		Type 4507	2195936	Ch. 3: B Pillar Striker
			2195937	Ch. 2: B Pillar Lower Top
2203551	Ch. 1: B Pillar Top			
Digital Protractor	Lucas	model DP45	41110023	
Force Gauge 1kN	Mark-10	M5-200	3461570	to not damage the car, a steel interlayer has been applied
Car Door Velocity Sensor	Newport	P61A	1100104-00	

Table 3.2.: Equipment used during the sound pressure level and vibrational measurements.



## 4. Measurement Results

Within the following chapters, the results of the acoustic camera measurements and those of the measurements using the classical approach are analyzed and discussed in detail.

### 4.1. Acoustic Camera

The results of the acoustic camera measurements are presented in this chapter. Due to the high amount of pictures taken during these measurements, only the most important ones are presented here. All results focusing on the area around the B-Pillar can be found in the Appendices A.1 and A.2. Also, one needs to note that the pictures within this chapter are presented with a fixed dB(A)-scale in order to show the pressure-relations between different measurement positions. As a result of this, the statements of the pictures were slightly influenced. Significant level differences are not detectable anymore, due to coarseness of the level scale. Thus, all results in the appendix are presented without the adjusted dB(A)-scale. The scale there is depending on the maximum and the minimum occurring sound pressure level within a range of 8 dB.

#### 4.1.1. Reliability of the Camera

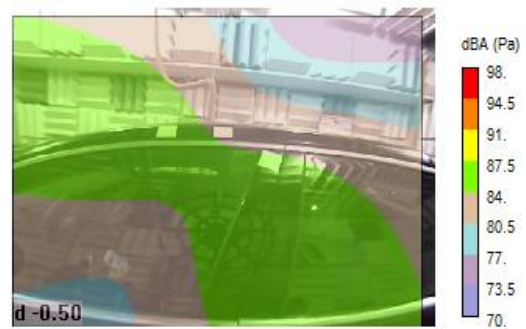
In order to ensure a certain repeatability of the measurements using the acoustic camera, and thus to prove the reliability of this measurement device, two different cars have been tested under the same conditions. The results can be seen in the following Pictures 4.1(a) - (f) and 4.2 (a) - (f), as well as in Figures 4.3 (a) - (f) and 4.4 (a) - (f). Two different positions of the camera have been chosen, each sorted according to the frequency range covered by the pictures. They are showing the direct comparison of the two different cars, with car 1 being presented on the left column and car 2 on the right column.

*Position: Upper Rail Right*

As it can be seen in Pictures 4.1(a) - (f) and 4.2 (a) - (f), the results of the measurements on both cars are very similar when one is looking at the locations of the sources. This is especially the case for frequencies from 920 Hz to 1760 Hz. Here, the sources are located almost exactly at the same point, at the upper rail, close to the junction to the B-pillar. From 600 Hz to 880 Hz, the source locations are comparable, but not always



(a) Car 1: 600 - 680 Hz



(b) Car 2: 600 - 680 Hz



(c) Car 1: 720 - 880 Hz



(d) Car 2: 720 - 880 Hz

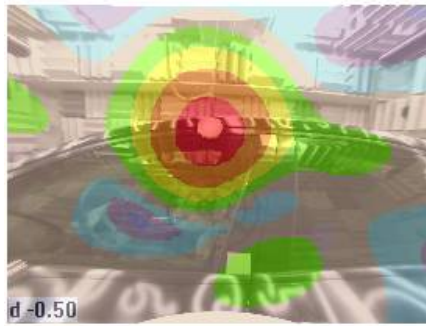


(e) Car 1: 920 - 1120 Hz

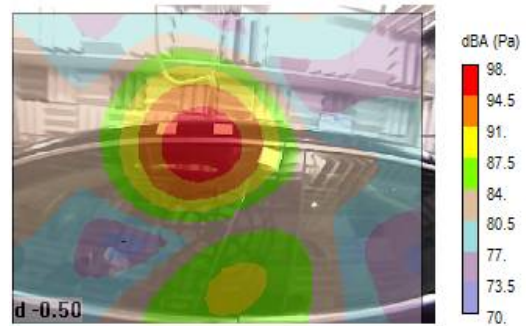


(f) Car 2: 920 - 1120 Hz

Figure 4.1.: Comparison of acoustic camera results at position Upper Rail Right, 600 - 1120 Hz



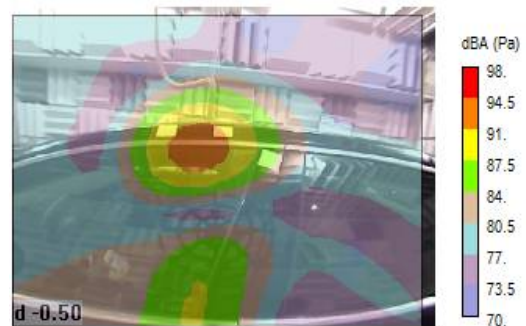
(a) Car 1: 1160 - 1400 Hz



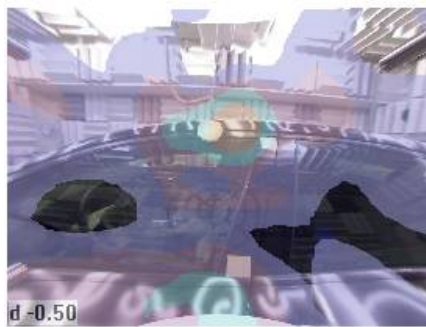
(b) Car 2: 1160 - 1400 Hz



(c) Car 1: 1440 - 1760 Hz



(d) Car 2: 1440 - 1760 Hz



(e) Car 1: 1800 - 2240 Hz



(f) Car 2: 1800 - 2240 Hz

Figure 4.2.: Comparison of acoustic camera results at position Upper Rail Right, 1160 - 2240 Hz

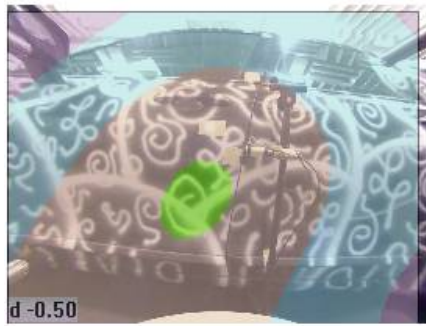
at the same position, see Figures 4.1(a) - (f) and 4.2 (a) - (f). This is mainly due to the fact that the camera reliability decreases, the lower the frequency range of observation is chosen, caused by the change of the spacial resolution. As calculated before, the resolution in this frequency ranges is rather poor in comparison to the higher frequencies. Also in the higher frequencies, from 1800 Hz to 2240 Hz, slight differences appear when it comes to the position of the sources. This can be a sign of a higher background noise or, which is more likely the problem in this case, the level difference  $\Delta L$  between the main lobe and the side lobes. As mentioned before, the quality of the measurement results decreases while increasing the frequency. For an array with 36 microphones, a maximum frequency of 10000 Hz can be estimated. However, due to the reduction of 8 microphones, this frequency limit also decreased significantly which then caused the fact, that  $\Delta L$  is too low in order to neglect side lobes. In this case, the main lobes are still distinguishable from the side lobes, however, 2240 Hz now needs to be set as the higher frequency limit.

Radiating noise level-wise, the results of both cars are also comparable. The appearing sound pressure levels are sufficiently close to each other. However there are slight differences, which are mainly caused by the fact that the displayed results are averages of single measurements within this particular bandwidth. Thus, small level differences can add up and change the overall result of the frequency band significantly. The relative differences between the sound pressure levels at the different positions on the door are comparable and thus reliable as presented in Pictures 4.2 (a) and (b). The highest sound pressure levels are measured at the Upper Rail for frequencies from 1160 Hz to 1400 Hz.

Another interesting result is, that the camera seems to be most reliable in the middle of the picture. Close to the edges, the location of the sources is rather difficult, as it is out of the view of the camera, although the device still recognizes sound radiating from that particular direction. Examples for this can be seen in Figures 4.1 (a) to (d). This can be a sign for different sound sources outside the field of view, influencing the camera again by varying time delays between the microphones.

*Position: B Pillar Lower Rail Right*

Figures 4.3 (a) - (f) and 4.4 (a) - (f) show, that the results of the two measurements are quite comparable. Here the Lower Rail Right, the results within the frequency range from 720 Hz to 1760 Hz are similar, both in locating the sources and when comparing the maximum levels. For frequency bands below and above this range, the observations from above can be found as well, looking at the different source locations in pictures 4.3 (a), (b), 4.4 (e) and (f) and their different level maxima. This is basically also the case for the results of the measurements at the other positions, see Appendix A.1 to A.2. The



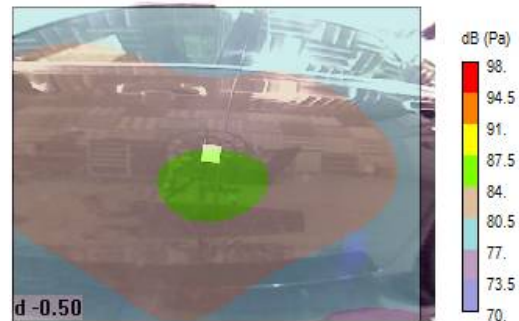
(a) Car 1: 600 - 680 Hz



(b) Car 2: 600 - 680 Hz



(c) Car 1: 720 - 880 Hz



(d) Car 2: 720 - 880 Hz



(e) Car 1: 920 - 1120 Hz

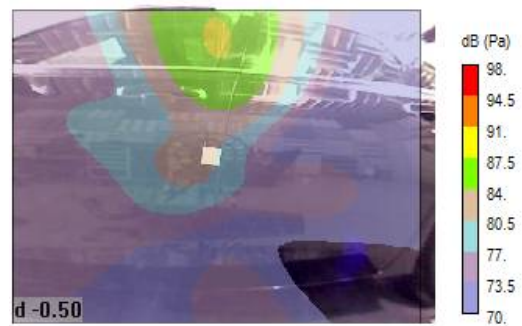


(f) Car 2: 920 - 1120 Hz

Figure 4.3.: Comparison of acoustic camera results at position B Pillar Lower Rail Right, 600 - 1120 Hz



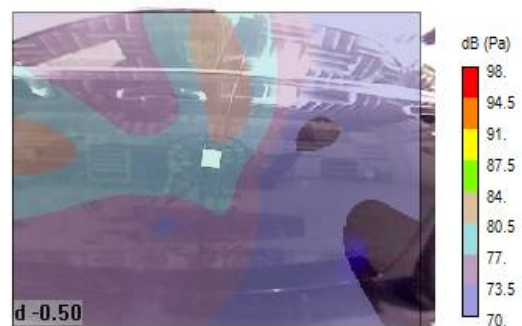
(a) Car 1: 1160 - 1400 Hz



(b) Car 2: 1160 - 1400 Hz



(c) Car 1: 1440 - 1760 Hz



(d) Car 2: 1440 - 1760 Hz



(e) Car 1: 1800 - 2240 Hz



(f) Car 2: 1800 - 2240 Hz

Figure 4.4.: Comparison of acoustic camera results at position B Pillar Lower Rail Right, 1160 - 2240 Hz

highest sound pressure levels can be recognized frequencies from 1160 Hz to 1400 Hz.

Thus, it can be concluded that repeatability of the measurements using an acoustic camera is possible. A sufficient reliability has been stated due to the repeatability of the measurement results.

#### 4.1.2. Location of the Sound Sources on the Car Door

Main task of the measurements of the acoustic camera was to identify the most important sources on the car door within the chosen frequency limits. From the Figures 4.1(a) - (f) and 4.2 (a) - (f), as well as in Figures 4.3 (a) - (f) and 4.4 (a) - (f) and those presented in the Appendix A.1, the two main sources of each frequency band have been identified and are presented in Table 4.1.

Frequency Range	Primary Source	Secondary Source
600 Hz - 680 Hz	Striker	Upper Rail Right / Frame Top
720 Hz - 880 Hz	Striker	Upper Rail Right
920 Hz - 1120 Hz	Upper Rail Right / Frame Top	Striker
1160 Hz - 1400 Hz	Upper Rail Right / Frame Top	Striker / Lower Rail Right
1440 Hz - 1760 Hz	Upper Rail Right / Frame Top	Striker
1800 Hz - 2240 Hz	Upper Rail Right / Frame Top	Striker

Table 4.1.: Main sources on the front door measured with the acoustic camera.

As one can see, the two most common sources identified with the acoustic camera are the Striker and the Upper Rail Right/Frame Top, these two types of sources appear nearly in every picture. Other sources are not displayed or have a rather low sound pressure level in comparison to the ones presented, for example the sources measured close to the A Pillar, see Appendix A.1. However, the location and the identification of the Upper Rail Right is a rather interesting result. This can be a sign for a local stiffness variations of the frame itself, or the door seal or it can be caused by vibrations of the glass of the window and needs to be further investigated. Nevertheless, the reliability tests of Chapter 4.1.1 confirm the measurements and show that the sound source at the Upper Rail is not a phenomenon appearing on one particular car. It more likely seems to be a typical property of this product. As stated above, the highest sound pressure levels appear between 1160 Hz and 1400 Hz for both positions and in general for the whole door. However, the displayed sound pressure levels at the striker are significantly lower than those at the Upper Rail. In fact, both source contributions can be seen in Figure 4.4 (b), showing clearly, that the sound pressure level of the striker is relatively lower. This leads to the assumption, that the overall sound perception is dominated by

the Upper Rail within this frequency range.

In summery, it is possible to conclude that the acoustic camera can be applied for measurements of this type, although the source(s) show a transient, impulsive signal. The results measured can be used to create a first estimation of the distribution of sound radiating sources across the door and to spot important hot-spots of sound radiation for later use. As a result, the classical approach have been chosen accordingly in order to confirm the measurements of the acoustic camera.

It is necessary to note, that it is not possible to clearly identify a source at the Frame Top as expected, since the position is located very close to each other. Due to the spatial resolution or certain algorithms of the software, a second source positioned at the Frame Top might have been overlapped by the one presented in the pictures. This also needs to be investigated further. However, in this case the acoustic camera should be only presenting the most dominant one.

Typical sound pressure levels for the primary sources are around 85 dB(A) at frequencies from 600 Hz to 880 Hz and from 1800 Hz to 2240 Hz, and 92 dB(A) to 97 dB(A) at frequencies from 920 Hz to 1760 Hz. For the secondary sources typical values range from 82 dB(A) to 86 dB(A), see Appendix A.1.

Finally, the acoustic camera can be a powerful tool to get an initial, quick image of the sound sources appearing on the object of investigation at certain, well defined positions, and in order to plan further measurements. However, for a detailed overview, various measurements need to be conducted in order to deal with the limitations given by the methods applied, such as the limited frequency range. The analysis then also needs to be very detailed and thus time consuming.

## **4.2. Classical Approach**

The results of the vibration and acoustical measurements are presented and discussed within this chapter. Due to the high amount of data it is not possible to present all graphs. Only the main results are shown, the remaining figures are attached in the appendix.

### **4.2.1. Reliability of the Classical Approach**

Several measurements and comparisons have been carried out in order to ensure the repeatability of the measurements.

*Repeatability of the measurements:*

As highlighted in Chapter 3.3, various boundary conditions needed to be fixed in order to assure a certain reliability. In order to verify the repeatability, four measurements, of which pairs of two had the same door velocity, namely 0.95 m/s and 1.01 m/s, have been chosen and compared directly to each other. The results can be found in Figure 4.5 and 4.6. For the acoustic head, the results of both microphones for one measurement were averaged.

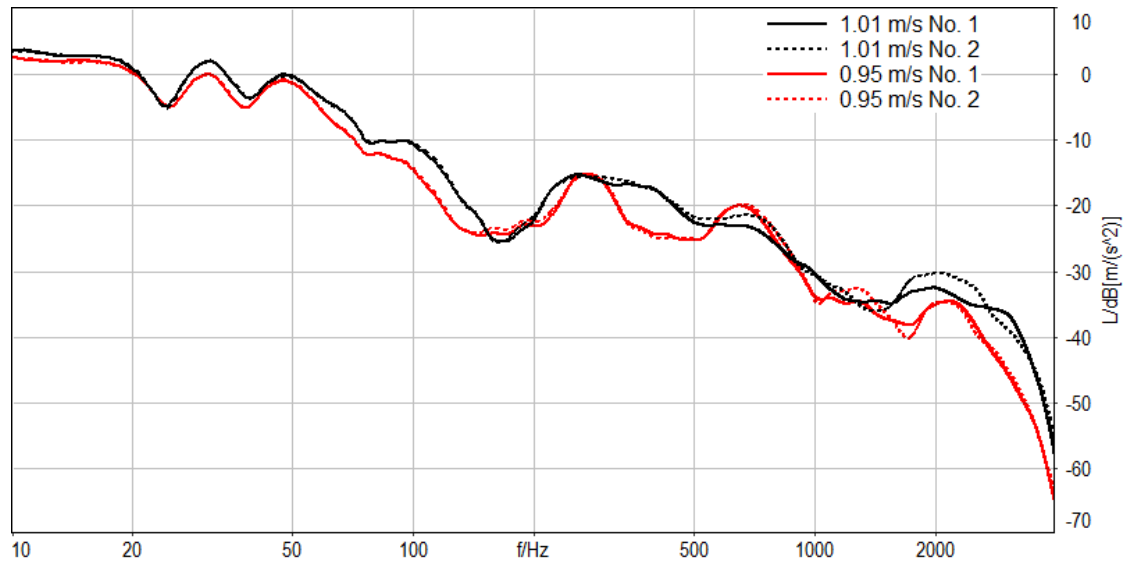


Figure 4.5.: Comparison of the accelerometer levels of four independent accelerometer measurements. Position: Frame Top

As shown in Figure 4.5, the results of all accelerometer measurements are very similar when comparing them to the measurement of the same door closing velocity. The results correspond with each other, especially in the lower to medium frequencies, from 10 Hz until 1000 Hz. Above 1000 Hz, slight differences can be found. However, this is a typical observation, as higher frequencies can be more likely influenced by uncertainties, such as environmental influences.

In Figure 4.6, one can recognize the matching results of the sound pressure levels of the corresponding door closing velocities. Here, the results are very comparable, only at certain frequencies, slight differences of 2 dB can be found. However, these can be caused due to the averaging of the results of the left and the right microphones. Overall, repeatability was proven at every measurement position. Thus, the results are reliable among each other.

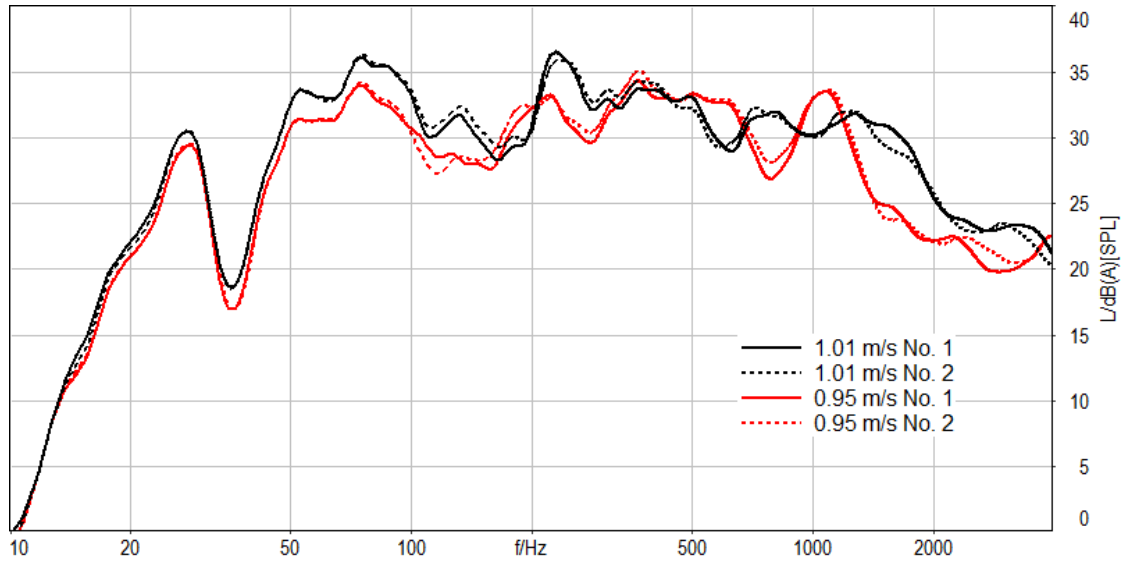


Figure 4.6.: Comparison of the sound pressure levels of four independent acoustic head measurements

*Velocity range of the door:*

As described before, the door closing velocity range also needed to be fixed since it is not effective to focus only on one particular velocity. It is very difficult to always achieve the same speed while manually closing the door. Thus, the velocity range was limited to 0.97 m/s - 1.03 m/s. Several initial measurements with different velocities have been carried out in order to show the reliability of this chosen range. The results of the comparison of the different velocities for one accelerometer and the sound pressure level, averaged over the left and the right microphone, are presented in the following Figures 4.7 and 4.8. A velocity range of the same width of 0.06 m/s, from 0.98 m/s to 1.04 m/s is covered.

As it can be seen in Figure 4.7 and 4.8, the variations between the different velocities are rather small. Again, the results are very comparable and close to each other in a frequency range from 10 Hz to 200 Hz. Higher than that, slightly higher level differences appear. The maximum  $\Delta L$  is here 5 dB for the sound pressure level at about 1200 Hz. These differences are basically caused by the changing force input into the door while closing the door. As described above, even small velocity changes matter significantly. Since the author always carried out three measurements per setup, it was ensured that a measurement within the described velocity range was chosen for analysis.

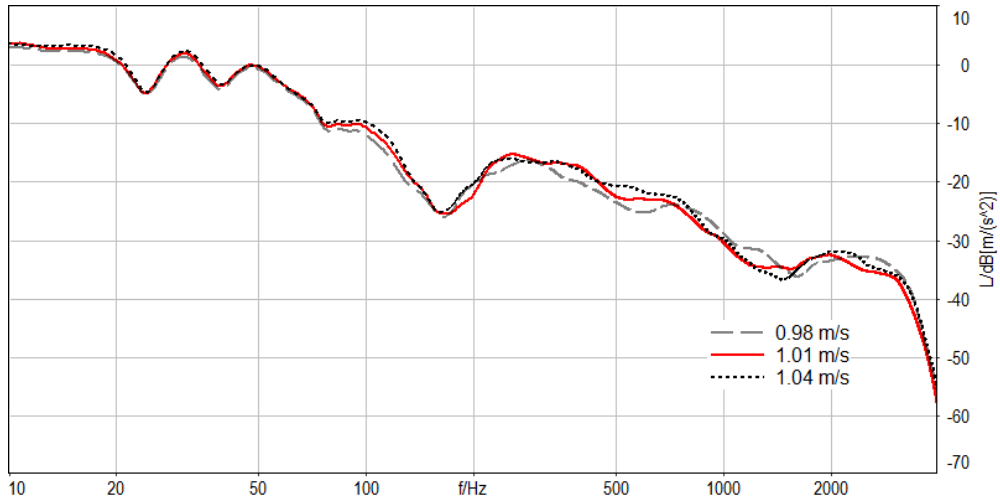


Figure 4.7.: Comparison of the accelerometer levels of three different velocities. Position: Frame Top

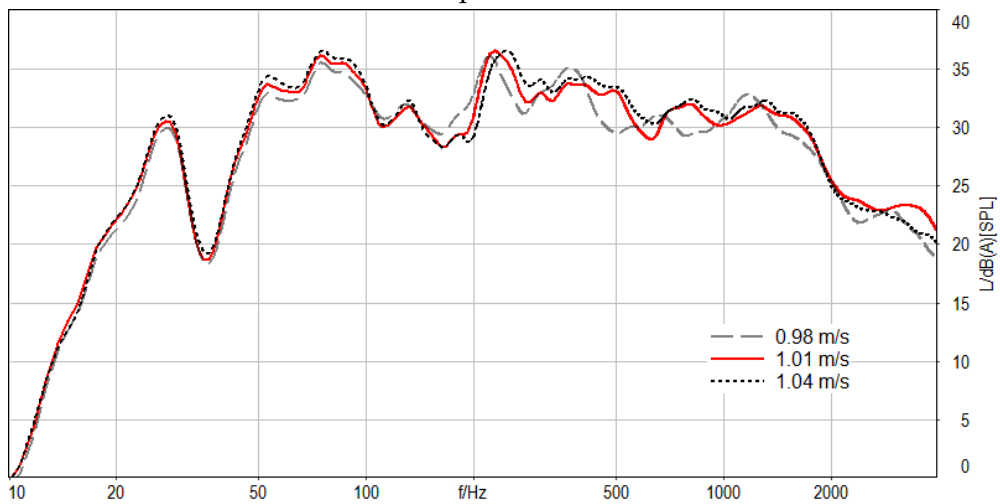


Figure 4.8.: Comparison of the sound pressure levels of three different velocities using the acoustic head

*Coherence:*

One possibility to verify a high transmission of vibrations to airborne sound is to analyze the coherence between the levels measured by an accelerometer and a microphone. A high coherence, for example of 100 %, then means, that the vibrational energy is directly transformed into acoustical energy, whereas a low coherence could either stand for the opposite or the influence of high background noise. This is usually the case for higher frequencies. In order to ensure results of good quality, the coherence of one particular setup has to be calculated for various measurements and then needs to be av-

eraged. Therefore, 10 to 20 measurements are typically averaged. However, due to the strict time planning for this project, it was only possible to measure and average over 3 different measurements for one setup (and position). Thus, results of low coherence in higher frequencies were expected. The results for two exemplary coherences can be found in Figure 4.9. The coherence between the Striker and the sound pressure level of the left microphone, and between the A Pillar and the sound pressure level of the left microphone are presented. The results of the remaining accelerometers in comparison to the levels of the left microphone were generally equivalent to those of the ones presented.

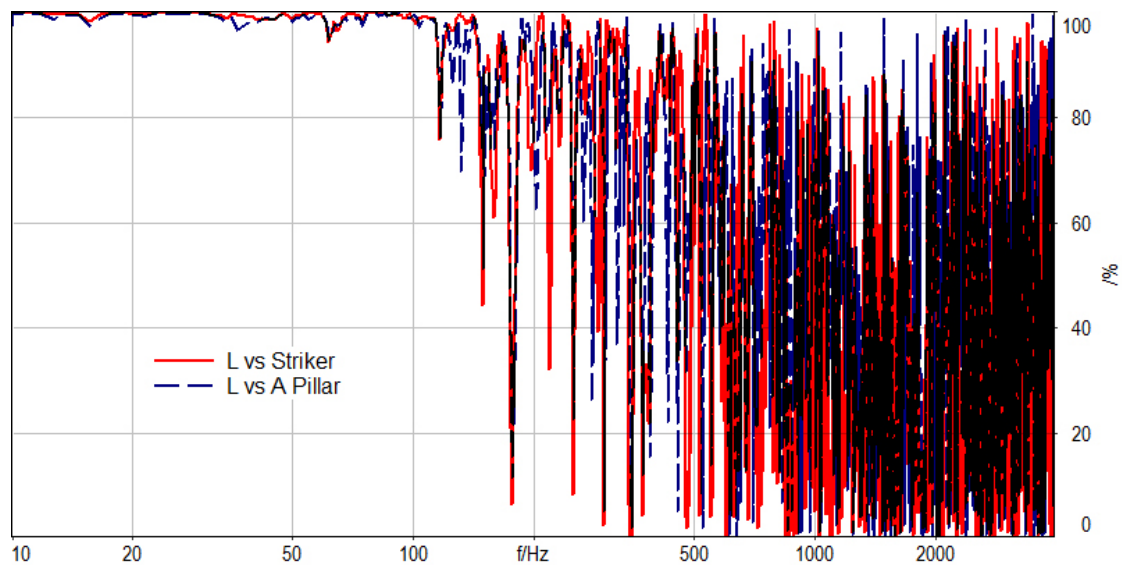


Figure 4.9.: Comparison of the coherences of the Striker and the A Pillar with the left microphone, averaged over three measurements

The results of the coherences presented can basically be split into three different frequency regions. From 10 Hz to 100 Hz, generally a high coherence of almost always 100 % can be recognized. This basically means that changes of the vibrations within this range will change the sound pressure level very likely. Only exceptions appear for the Frame Top at frequencies of 25 Hz and 86 Hz. At 86 Hz, the coherence of the Upper Rail Right also has a slight dip. There, the influence of changes of vibrational levels will not be such significant. The second region can be defined to range from 100 Hz to 500 Hz with coherences close to 100 %. There, a high transfer can be expected, however, it is also already influenced significantly by uncertainties, such as the background noise. Above 500 Hz, the coherence hardly ever is equal to 100 %, only in exceptions. Here, the signal will be most likely influenced by uncertainties, which basically also confirms

the lower reliability of measurements taken in higher frequency ranges. However, as mentioned before, this kind of results was already expected due to the low amount of measurements averaged.

#### 4.2.2. Transfer Functions

Another possibility to analyze the influence of structural vibrations on an acoustic signal is to calculate the transfer functions. Like the coherence, two signals are compared to each other, the input level and the output level. In Figure 4.10, the transfer functions of all accelerometer levels are set in relation to the sound pressure level of the left microphone. Here, the accelerometer levels were set as inputs and the sound pressure level of the left microphone as output. The results of these relations can be understood as a sort of amplification factor for every frequency of the measured levels. Similar input and output signals are less amplified in comparison to those with a high output and a lower input level and vice versa.

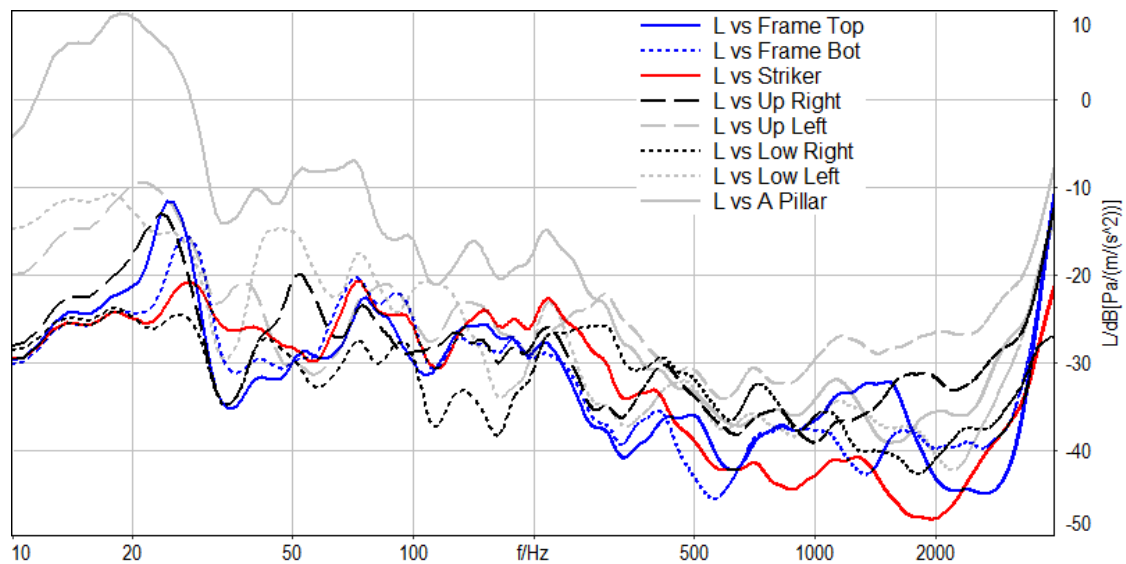


Figure 4.10.: Comparison of the transfer functions of all accelerometer level in relation to the left microphone

A high value of the transfer function can basically stand for two alternatives. The first one describes low transformation from vibrational to acoustical energy since the level of vibrations, the input level, in comparison to the sound pressure level (output) is not significantly high enough and thus negatively amplified. Figure 4.10 for example shows, that the transfer function of the A Pillar has the highest values at frequencies from 10 Hz to 270 Hz, also those of the Upper Rail Left and the Lower Rail Left nearly always show high values in comparison to the other transfer functions. This basically

confirms the expectations explained above, stating, that the door closing sound is rather less influenced by the region close to the A Pillar than of that of the striker and the B Pillar. On the other hand, high values of the transfer function can also represent higher changes within the sound pressure levels in comparison to relatively small variations of the vibrational levels.

A low value of the transfer function on the other hand can describe the exact opposite. Either, the vibrational levels are generally low in comparison to the sound pressure level or the changes of the sound pressure level are more significant than those variations of the vibrations. This could then mean that a minor change in vibrations at a certain position has a rather high influence on the radiated sound.

However, since it can be assumed that all vibrations across the door are highly correlated, a more detailed study needs to be carried out in order to identify clear sources of radiation for certain frequencies by studying both the levels of vibrations and the transfer functions.

In order to interpret the results of the transfer function analysis in Figure 4.10, the following results can be concluded, assuming that a high value of the transfer function represents a low influence and a low value of the transfer functions stands for a high influence of vibration on the sound pressure level: the most influencing position from 10 Hz to 30 Hz is the Lower Rail Right, from 30 Hz to 50 Hz the Frame Top, from 50 Hz to 200 Hz the Lower Rail Right, from 200 Hz to 450 Hz the Frame Top, from 450 Hz to 650 Hz the Frame Bottom, from 650 Hz to 2500 Hz the Striker and from frequencies higher than 2500 Hz the Frame Top. The least influencing positions are the A Pillar and the Upper Rail Left. These conclusions are partly confirmed by the results of the acoustic camera, stating that the Striker is the most active position at frequencies from 600 Hz to 880 Hz. Higher than that, the results do not match. This can be already a sign for low vibrational contribution to the sound pressure level at the Striker and the Frame Top at frequencies higher than 920 Hz.

However, these assumptions need to be cross-verified. This can be done by comparing the effects of stiffness changes on vibration and acoustical levels.

#### **4.2.3. Stiffness Variations at Several Positions**

The stiffness was varied at the main hot-spots, detected with the acoustic camera, namely the Striker, the Frame Bottom and the Upper Rail Right. Therefore, the door seals were compressed by placing tape on them. This increased the local density of the door seals at the mentioned positions. All in all, two different stiffness variations were tested: compressing with one and two layers of tape. The changes of the sound

pressure level, averaged over the left and the right microphone, can be found in Figure 4.11.

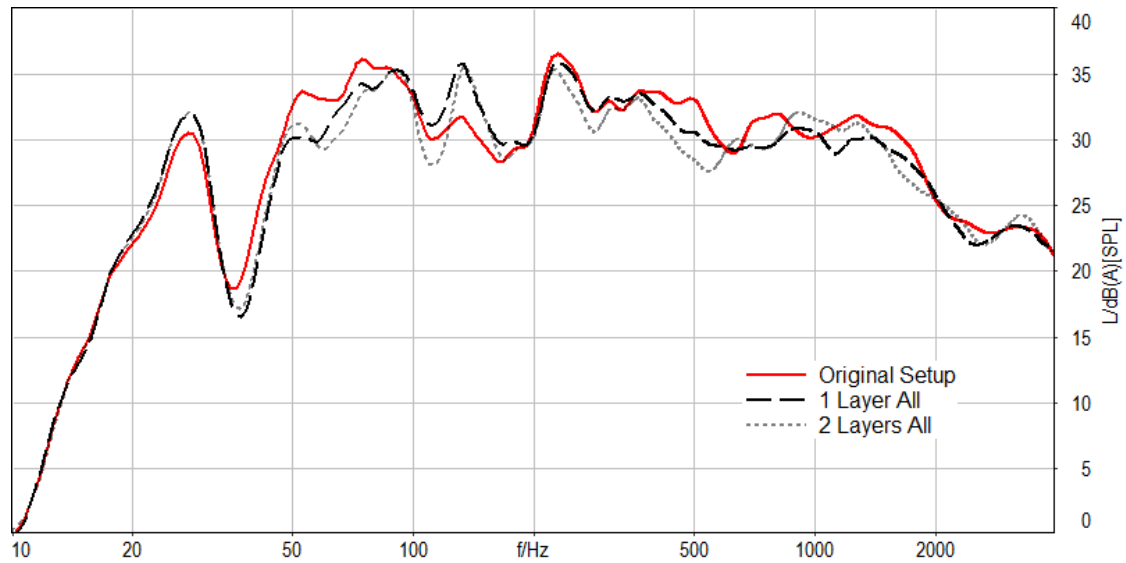


Figure 4.11.: Comparison of the sound pressure levels of the original setup and the stiffness variations.

As one can see in Figure 4.11, the sound pressure levels got reduced in most of the frequencies when applying one or two layers of tape at all hot-spots mentioned before. This can be deduced to damping caused by the increase of stiffness at the selected positions. An example for the changes of the accelerometer levels can be found in Figure 4.12. There, the measured vibrations at the Frame Top are presented. Most of the times, one layer is sufficient enough in order to achieve recognizable results in damping. In some cases, a second layer of tape even provoked a decrease in damping again. A reason for this behavior can be, that the second layer did probably not increase the local density further but decreased it by adding a softer layer, in this case tape, compared to the compressed seal.

However, the level was increased at frequencies at around 141 Hz and 925 Hz. Comparing the changes in sound pressure levels with those of the vibration levels, one can identify the areas of the door, which are contributing vibration-wise primarily and secondarily to the change of the sound pressure levels at specific frequencies. For example, within the frequencies of 141 Hz and 925 Hz, the Frame Top (141 Hz, see Figure 4.12) and the Striker and the Upper Rail Right (925 Hz) also show the highest changes in vibrations, see Appendix B.1 and Table 4.2. This also confirms partly the assumption of the previous Chapter 4.2.2, mentioning that the striker is active at around 925 Hz.

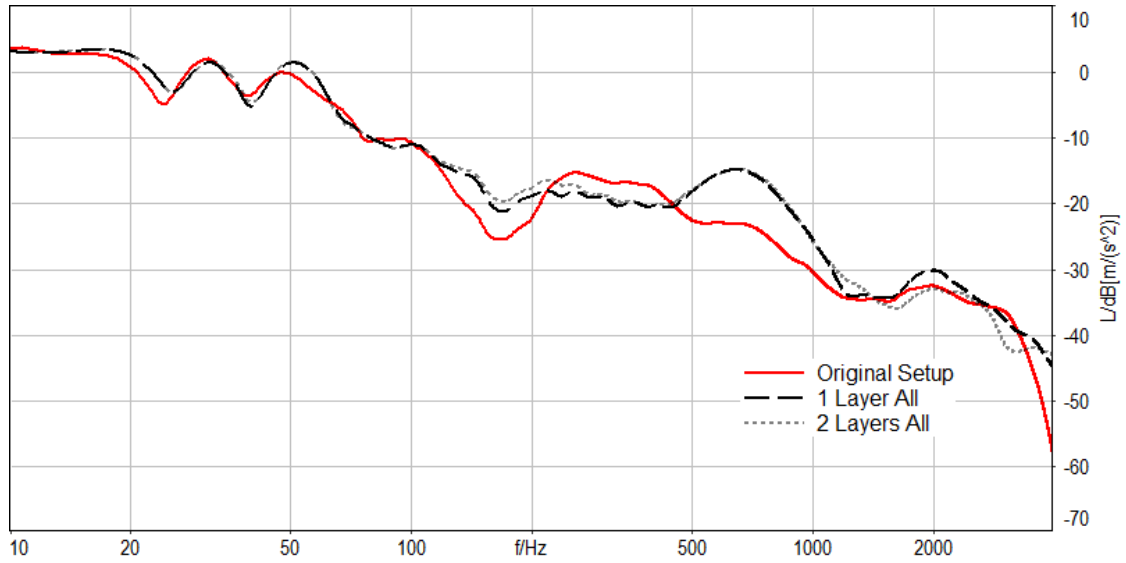


Figure 4.12.: Comparison of the accelerometer levels of the original setup and the stiffness variations. Position: Frame Top.

However, the other two contributors were not confirmed. A more detailed overview of the main and secondary contributors to the changes of the sound pressure level can be found in Table 4.2. There, vibrations that caused a remarkable change of the sound pressure level, in these cases by damping, were marked with the label “major”. Measurement positions not mentioned in this table have either no influence or supposedly a negative influence on the changes of the sound pressure level but are low enough to be ignored.

Frequency f [Hz]	Primary Source	Secondary Source	Influence
38	Striker	Lower Rail Right, A Pillar	
56	Upper Rail Right	-	major
86	Upper Rail Left, Lower Rail Right	-	
114	(Upper Rail Left)	Frame Bottom	
141	Frame Top	Upper Rail Right and Left	
163	Frame Top, Frame Bottom	Lower Rail Right, Upper Rail Right	major
280	Upper Rail Right	Frame Top, Striker, Upper Rail Left, Lower Rail Left	
500	Frame Bottom	Upper Rail Right	major
800	(Striker), Upper Rail Right	Lower Rail Right and Left, A Pillar, Upper Rail Left	
925	(Striker), Upper Rail Right	Lower Rail Left, Upper Rail Left	
1270	Frame Bottom	Lower Rail Right, Striker, Upper Rail Right and Left	
1900	Lower Rail Right, Upper Rail Left	Upper Rail Right	

Table 4.2.: Primary and secondary sources while applying layers of different stiffnesses.

As it can be seen in Table 4.2, the primary sources are always located around the B Pillar. Major influences appear at 56 Hz, caused by the Upper Rail Right, at 163 Hz,

caused by the Frame Top and Bottom, and at 500 Hz, caused by the Frame Bottom. The assumptions from Chapter 4.2.2, however, can not always be confirmed. In fact, only the dominance of the Striker at 800 Hz and 925 Hz can be proven. There, the relation of the sound pressure level to the vibrational level seems to be comparable. For the other frequencies it can be concluded that a direct relation of the output and the input signal can rather be expected at a transfer function level of roughly -25 dB at lower frequencies and of roughly -35 dB at higher frequencies. Also, one needs to note that the transfer functions confirmed the less influential measurement positions, as mentioned in Chapter 4.2.2.

The results of the acoustic camera are also partly confirmed. The camera measured a high sound pressure level of the striker at 800 Hz and of the Upper Rail Right at 925 Hz. There, the vibrations have major influence on the sound pressure level. The acoustic camera also predicted the secondary sources in most of the cases correctly. Differences can be again explained by the spatial resolution and the fact that the author decided to take averages over 3<sup>rd</sup>-octave bands. Thus, a wider frequency range is covered and averaged and the results can slightly differ. However, the tendency is correct and confirms again the applicability of the acoustic camera for this type of measurements. Further research should be performed, though, with respect to smaller frequency ranges in order to investigate the accuracy of the camera.

Overall, one needs to mention, that this type of stiffness variation is rather impractical. In reality, a local change of the stiffness is very difficult to implement and control, furthermore it also is not effective regarding costs. Also, for a better control of the stiffness variations it is necessary to actually quantify the applied material changes, such as the difference in density, etc. Thus, further research needs to be carried out within this field. However, as mentioned before, this thesis can be considered to be more likely a foundation for the idea to quantify door closing sound quality.

To draw a conclusion, the stiffness variations at the three hot-spots influenced the sound pressure and vibration levels significantly within specified frequency ranges by damping or increasing these levels. Thus it was possible to clearly define frequency ranges of the sound pressure levels, which were mostly influenced by radiation caused by vibration rather than due to airborne effects. The predictions of the transfer functions were partly confirmed, the same can be noted for the acoustic camera measurements.

#### **4.2.4. Stiffness Variations at Single Positions**

With respect to the results of Chapter 4.2.3, an allocation of the most influencing local stiffness variation to a certain frequency and a certain measurement position would be

interesting, especially for the three major sound pressure level changes at 56 Hz, 163 Hz and 500 Hz. Therefore, each one of the three stiffness variations has been tested independently by compressing the door seal locally with one layer of tape. By comparing the achieved vibration changes at a certain point of measurement with those of Chapter 4.2.3, one can formulate hypotheses about which one influenced that certain position the most in a certain frequency range. Thus, the most important findings have been summarized in Table 4.3.

Frequency f [Hz]	Influenced measurement position:	Influenced most by a stiffness variation at:	Notes
56	Upper Rail Right	Frame Bottom	major
163	Frame Top	Striker	major
	Frame Bottom	Frame Bottom	major
220	Upper Rail Left	Upper Rail Right	
280	Frame Top	Frame Bottom	
	Upper Rail Right	Striker	
	Upper Rail Left	Frame Bottom	
	Lower Rail Left	Frame Bottom	
480	Upper Rail Left	Frame Top	
500	Frame Bottom	Frame Top	
	Upper Rail Right	none of these three changes	major
800	Frame Top	Frame Top	
	Lower Rail Left	none of these three changes	
1270	Frame Bottom	Frame Top & Frame Bottom	

Table 4.3.: Single stiffness variations as main influences on vibration variations.

Since it is hypotheses, only the major influences are being described further. The first major change in the sound pressure level, recognized at 56 Hz can be mainly allocated to the Upper Rail Right. The main vibration changes at this position was achieved by a local stiffness change at the Frame Bottom.

A direct comparison of the vibration levels at this position can be found in Figures 4.13 and 4.14. All other results are attached in the appendix.

Another example, supporting this hypothesis, is the change of vibrations for the Upper Rail Right at 280 Hz. When looking at the accelerometer levels of the single variations in Figure 4.14, the stiffness alteration at the Striker caused the main decrease of the vibration level, achieving a comparable level reduction. An explanation for the fact that this type of divergence at 280 Hz is recognized at the Upper Rail Right instead of at the Striker, where stiffness was actually changed, it can be that the door is connected rather rigidly to the frame at the Striker position as soon as the door gets closed. Thus, it would rather work like a joint. By changing the stiffness (and due to that the density of the material) locally, the rotations around the joint are damped due to the harder

surface, this then also results in less vibrations at the Upper Rail Right.

However, since these are hypotheses it would be necessary to investigate this topic further in the future.

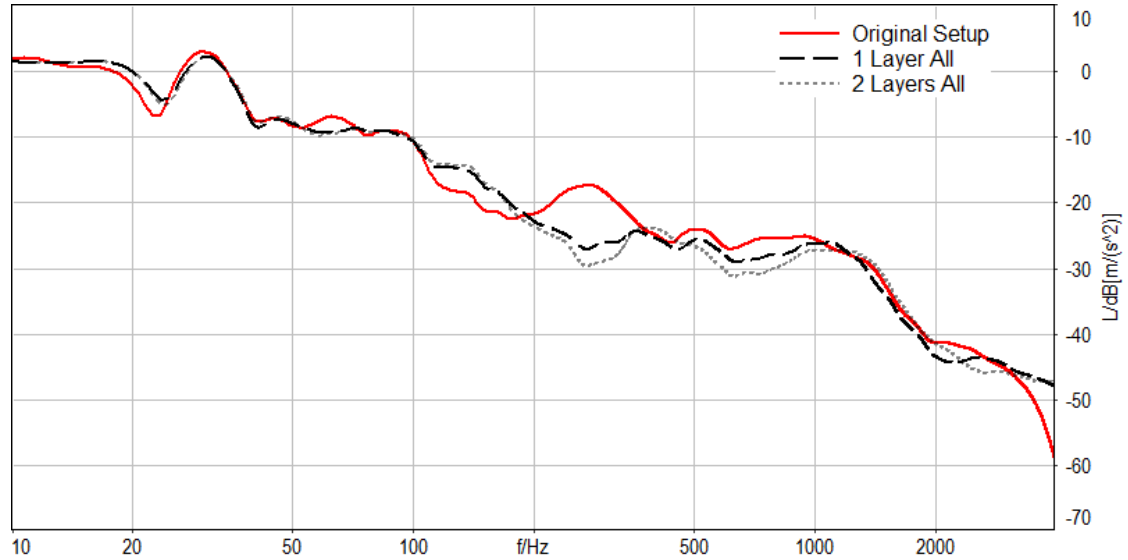


Figure 4.13.: Changes of vibrations due to stiffness variations at three positions, depending on the amount of layers applied. Position: Upper Rail Right.

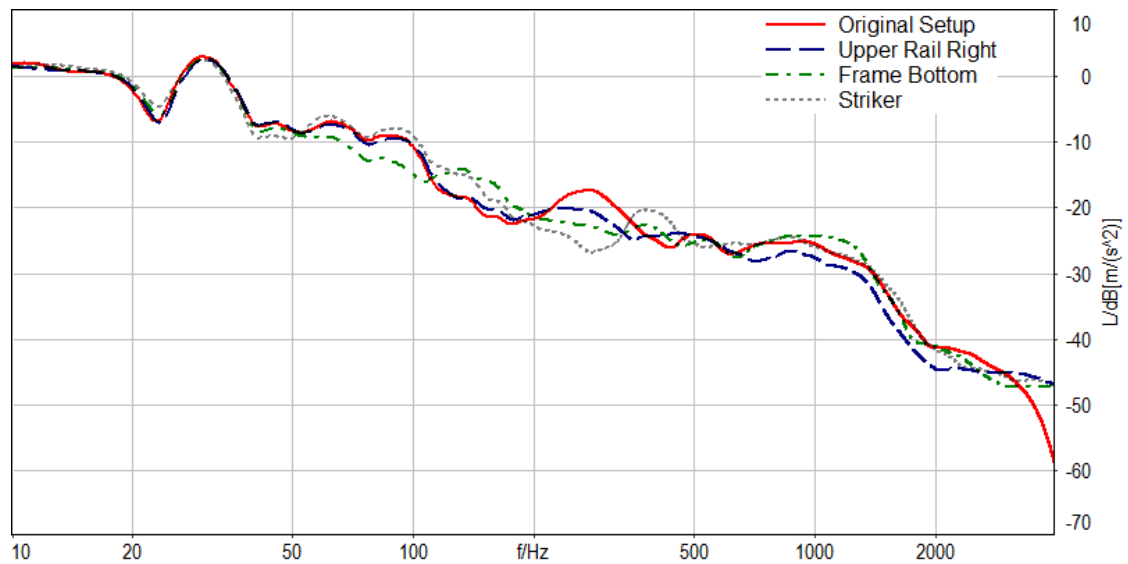


Figure 4.14.: Changes of vibrations due to stiffness variations at single positions. Position: Upper Rail Right.

#### 4.2.5. Varying the Inclination of the Car

The second parameter of investigation was the inclination of the car. Therefore, several measurement rows were conducted while lifting the car from the left, the right, the front and the back by  $0.5^\circ$  and  $1.0^\circ$ . A comparison of the sound pressure levels for the inclination from the left and the right can be found in Figure 4.15.

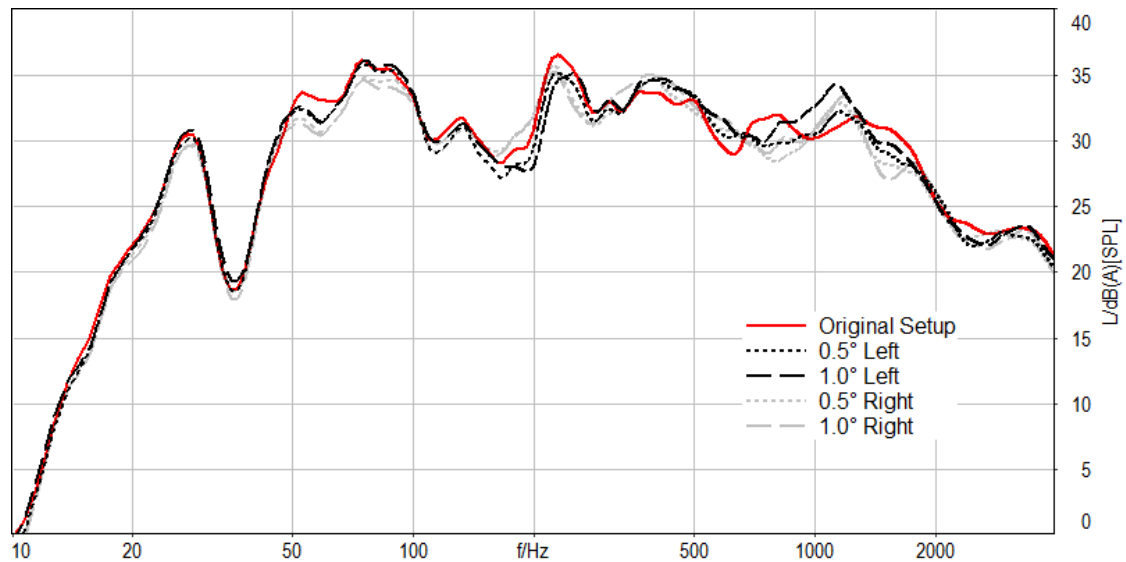


Figure 4.15.: Comparison of the sound pressure levels while lifting the car from the left and the right at different angles.

As shown in Figure 4.15, the sound pressure level is mainly influenced by the variations of inclination at four different frequencies: at 55 Hz damped by the Lower Rail Left and Right, at 200 Hz caused by Lower Rail Right and at 1520 Hz damped by the Frame Top and Bottom, the Upper Rail Left and partly also by the Striker. At 790 Hz it seems that the vibrations at almost every measurement position are influencing the sound pressure level by damping, except the Upper Rail Right. At frequencies of 400 Hz, 480 Hz, 620 Hz and 1126 Hz a clear identification is not possible. Furthermore it is necessary to note that also a clear classification of primary and secondary sources is not possible. This can be connected to the following fact: In comparison to the stiffness variations, where only local changes have been applied, the inclination of the car influences the whole body including the door. Thus, one can recognize changes of vibrations at more positions on the door. In fact, even measurement locations which were rated to be not as influential as the main ones, such as the A Pillar and the Upper and Lower Rail Left seem to be radiating and thus influencing the sound pressure level more. These results can be found in the following Table 4.4.

It is also not always possible to determine main sources for increasing sound pressure levels since the vibration levels at these particular frequencies either are damped or equal to those of the original setup.

Frequency $f$ [Hz]	Main Sources	Notes
55	Lower Rail Left and Right	major
86	-	No change in vibration levels detectable!
114	Upper Rail Right	
163	Frame Bottom	
200	Lower Rail Right	major
260	Frame Top and Bottom, Lower Rail Right	
400	-	No change in vibration levels detectable!
480	(A Pillar, Striker, Lower Rail Left)	No major change in vibration levels detectable!
620	(Striker, Upper Rail Left)	No major change in vibration levels detectable!
790	A Pillar, Striker, Lower Rail Left and Right, Upper Rail Left and Right, (Frame Top)	major
1126	(Upper Rail Right and Left)	No major increase in vibration levels detectable!
1520	Frame Top and Bottom, Upper Rail Left, Striker	major

Table 4.4.: Main sources while applying left and right inclination to the car.

The variations of the sound pressure level due to the inclination of the car from the back and the front can be found in Figure 4.16. A corresponding determination of the main sources can be found in Table 4.5.

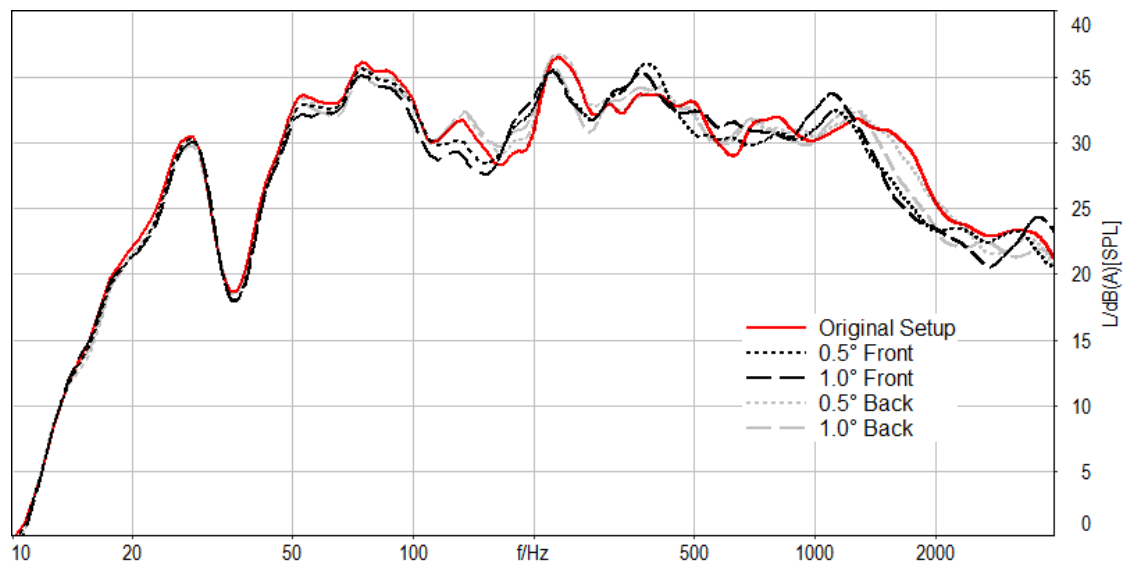


Figure 4.16.: Comparison of the sound pressure levels while lifting the car from the front and the back at different angles.

In Figure 4.16, three frequencies of major sound pressure level changes due to the vari-

Frequency f [Hz]	Main Sources	Notes
55	Frame Top, Lower Rail Left	
86	Striker, Lower Rail Right and Left	
114	Frame Top, Striker, Lower Rail Right and Left, Frame Bottom	major
141	Striker, Lower Rail Left and Right, Upper Rail Left and Right, Frame Top	
180	Frame Top	
230	Frame Top and Bottom, Lower Rail Right	
400	(A Pillar)	No major change in vibration levels detectable!
500	Frame Bottom, Striker, Upper Rail Left and Right, Frame Top, A Pillar, Lower Rail Left	
630	(A Pillar)	No major change in vibration levels detectable!
800	Striker, Lower Rail Left and Right, Upper Rail Left and Right	
1100	(Frame Top), Upper Rail Right	major
1600	Frame Top, Striker, Lower Rail Left, Upper Rail Left	

Table 4.5.: Main sources while applying front and back inclination to the car.

ations can be found. In this case, the sound pressure level is damped significantly at 114 Hz, caused by the inclination of the front side of the car and at 1600 Hz, again due to the change of the angle from the front side, and partly also from the backside. At 1100 Hz, the sound pressure level increased for both cases, however, it is not possible to find accelerometer levels showing a similar behavior. This can also be recognized for several other frequencies, where the sound pressure level increases.

In summary, the frequencies where variations can be found are comparable to those of the left and the right inclination. Only slight differences can be detected, which is a sign for frequency shifts, for example at 620 Hz, 790 Hz or 1126 Hz. Frequency shifts were not recognized during the analysis of the stiffness changes. Also, the main sources correspond to each other mostly.

An interesting phenomenon that appeared during the analysis of these measurements is the level difference of the the vibrations measured for the variations while comparing left, right, front side and backside inclination. Generally, the measured levels of the front and the backside are slightly lower than those of the left and the right side. Also, the levels of the vibration measurements of the left and the right side correspond to the levels of the original setup. This is especially the case for lower frequencies from 50 Hz to 500 Hz. Examples can be found in the Appendices B.3 and B.4. A reason for this can be the original inclination of the door, which was already implemented due to the design of the car. The door is slightly angled towards the car. Thus, a change of the angle in this direction should not influence the behavior of the door significantly. However, the door is less inclined towards the front or the backside. Thus, a newly introduced

additional angle will change the properties of the door closing behavior. This can also mean that the door closing effort, meaning the input power needed to close the door with a certain velocity might be influenced.

Overall, it was shown that the variation of the angle of the vehicle can have significant influence on the sound pressure level. It was either damped or increased, depending on the frequency of observation. Furthermore, slight frequency shifts were discovered as well. In order to evaluate the perception of these variations, it is necessary to carry out listening tests.



## 5. Summary and Conclusions

This thesis was split into two parts. One purpose was to get acquainted to and implement and test a new measurement technique for impulsive sound sources, which then should be verified by classical measurement methods. The second task was to investigate and measure the influence of stiffness and inclination variations on the door closing sound.

It was shown that the acoustic camera can be applied for short, impulsive sounds such as the door closing sound. The measurements were repeatable with a sufficient amount of accuracy. While analyzing the data, it was possible to determine various interesting locations on the door for later classical measurements using accelerometers and a binaural measurement system, highlighting that the Striker and the Upper Rail Right position, where most of the radiated sound was measured. The results of the acoustic camera were partly confirmed by those verifying measurements. Discrepancies can be explained by the method of averaging over 3<sup>rd</sup>-octave bands.

Variations of the stiffness and the inclination of the car clearly have an influence on the frequency contribution of the sound pressure levels and the vibration levels measured. For each variation, three main frequencies, namely 56 Hz, 141 Hz and 500 Hz ranges of high influence have been presented. The outcomes of the inclination investigations slightly differed from those of the stiffness variations. This is mainly due to the fact that the inclination alterations affected the whole structure of the car, whereas the stiffness changes only influenced local spots. Furthermore, slight frequency shifts were discovered while varying the angle of the car. In frequencies from 50 Hz to 500 Hz, vibrations are most likely influenced by lifting the car from the front or the back, rather than from the left or the right. Major influencing vibrations appear for left and right inclination at 55 Hz, 200 Hz, 790 Hz and 1520 Hz, for inclination from the front and the backside at 114 Hz and 1100 Hz.



## 6. Outlook

Considering the results and findings of this work, it is necessary to conduct further investigations and researches about this topic in the future. The applicability of the camera needs to be examined in detail in order to verify it as an independent measurement method and for this type of application and the level of detail of its' results. Therefore, a more detailed study needs to be carried out, investigating the measurement results using reasonable, finer frequency steps to average over.

Also, the influence of stiffness variations of the door should be investigated further. Key aspects would be the definition of stiffness variations as well as the measurement of its' influence on the door, while changing the stiffness of the whole seal at once.

Furthermore it is necessary to conduct listening tests evaluating the psycho acoustical influence of the parameters, treated within this project. Depending on the results, it would be a bit easier to quantify door closing sound quality.

Last but not least it also would be interesting to gain knowledge on how the door closing sound is actually perceived from the inside of a vehicle and whether this perception is influencing the customer while evaluating the perfect car to buy.



## References

- [1] Kuwano, S., Fastl, H., Namba, S., Nakamura, S. and Uchida, H.: *Subjective Evaluation of Car Door Sound*, Proceedings of the Sound Quality Symposium SQS, 2002.
- [2] Kuwano, S., Fastl, H., Namba, S., Nakamura, S. and Uchida, H.: *Quality of Door Sounds of Passenger Cars*, Proceedings of the ICA, 2004.
- [3] Törnqvist, H. and Wallin, S.: *Experimental investigation of mechanisms affecting the door closing sound of passenger cars*, Department of Applied Acoustics, Chalmers University of Technology, Göteborg, 2011.
- [4] Parizet, E., Guyader, E. and Nosulenko, V.: *Analysis of Car Door Closing Sound Quality*, Article at ScienceDirect, Elsevier Ltd., 2006.
- [5] Hamilton, D.: *Sound Quality of Impulsive Noises: An Applied Study of Automotive Door Closing Sounds*, General Motors Corporation, Traverse City, 1999.
- [6] Nayak, R. and Im, K.: *Optimization of the Side Swing Door Closing Effort*, General Motors Corporation, Detroit, 2003.
- [7] Kuo, E.Y. and Mehta, P.R.: *The Effect of Seal Stiffness on Door Chucking and Squeak and Rattle Performance*, Ford Motor Company, Detroit, 2004.
- [8] Sigl, J. and Scheucher, R.: *Acoustic Imaging of Sound Sources with a student-designed Acoustic Camera*, Department of Automotive Engineering, FH Joanneum University of Applied Sciences, Graz, 2007.
- [9] Christensen, J.J. and Hald, J.: *Beamforming, Technical Review No. 1 - 2004*, Brüel & Kjær, Nærum, 2004.
- [10] Grade, S, Hald., J. and Ginn, B.: *Noise Source Identification with Increased Spatial Resolution*, Brüel & Kjær, Nærum, 2004.
- [11] Wren, J.: *A Simple Frequency Response Function*, Prosig Noise & Vibration Blog, 2009.

- [12] Kropp, W.: *Propagation and Radiation of Structure Borne Sound*, Department of Applied Acoustics, Chalmers University of Technology, Göteborg, 2007.
- [13] *LMS Product Information - LMS/TL-ACT.78.2/11A*, LMS International, 2011.
- [14] *LMS Product Catalog - LMS Test.Lab Acoustics - Scalable Solutions for Spot-On Sound Testing and Analysis*, LMS International.





# A. Acoustic Camera Measurements

## A.1. Car 1

Figure A.1.: Position: Upper Rail Right

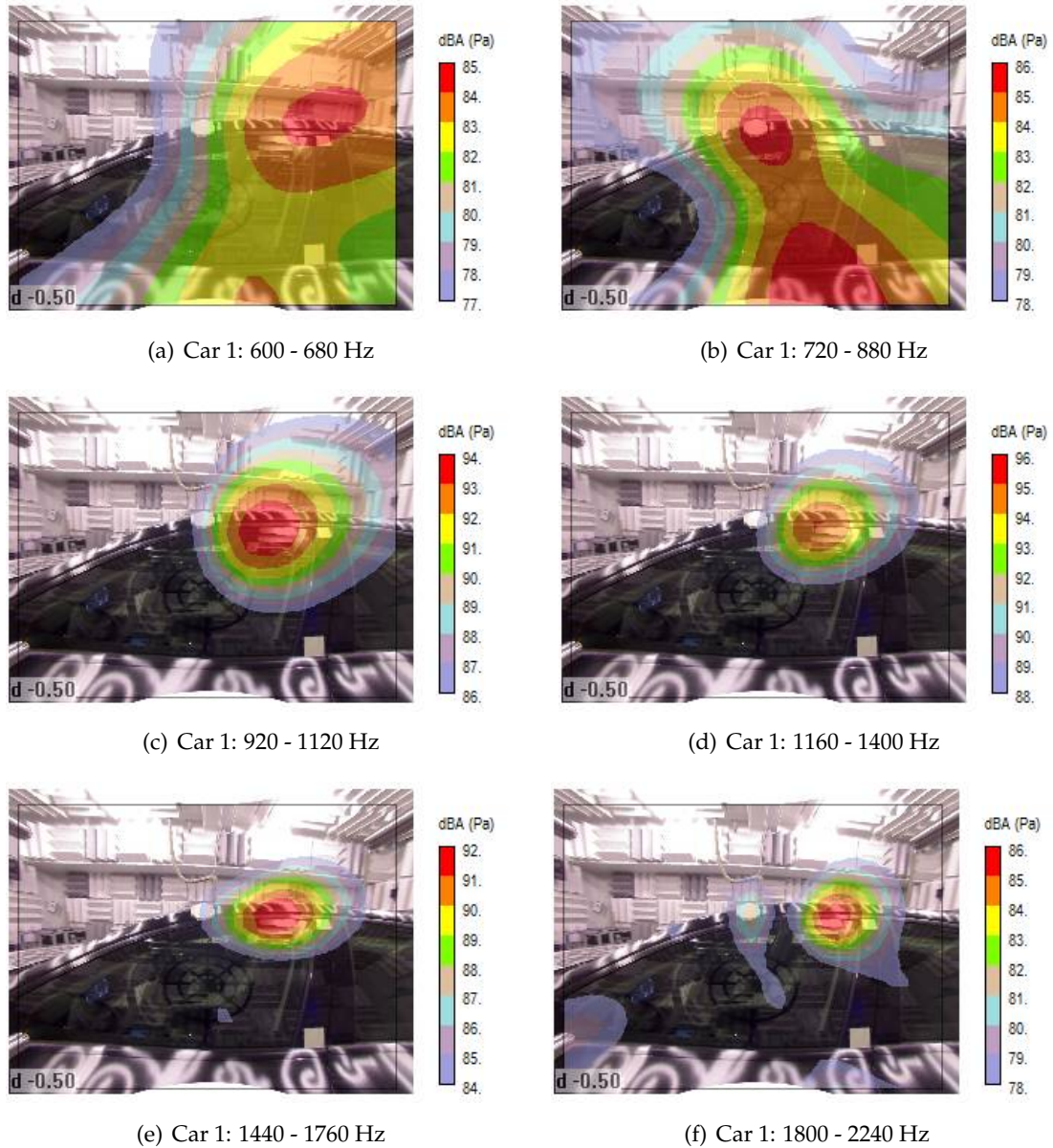
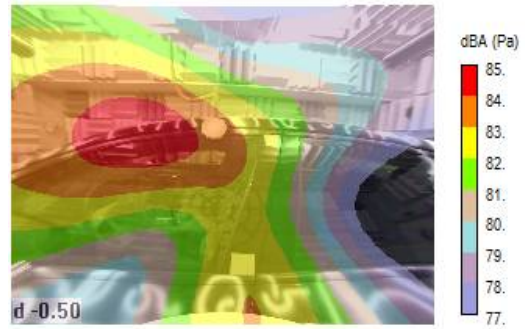


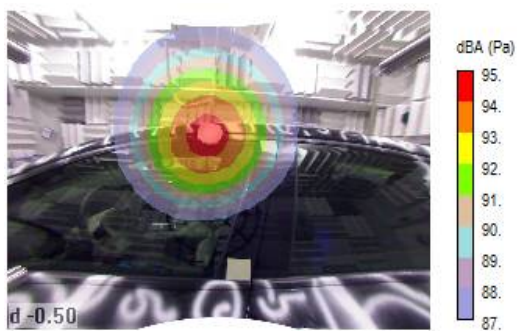
Figure A.2.: Position: Frame Top



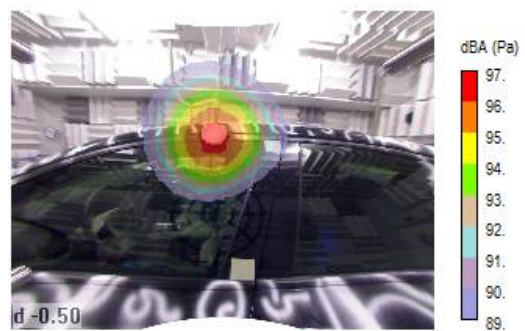
(a) Car 1: 600 - 680 Hz



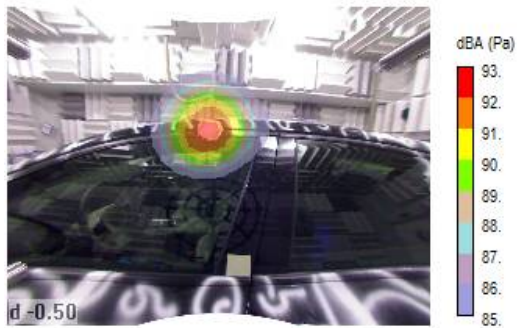
(b) Car 1: 720 - 880 Hz



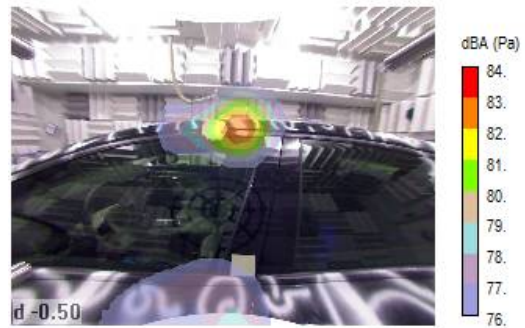
(c) Car 1: 920 - 1120 Hz



(d) Car 1: 1160 - 1400 Hz



(e) Car 1: 1440 - 1760 Hz



(f) Car 1: 1800 - 2240 Hz

Figure A.3.: Position: Frame Bottom



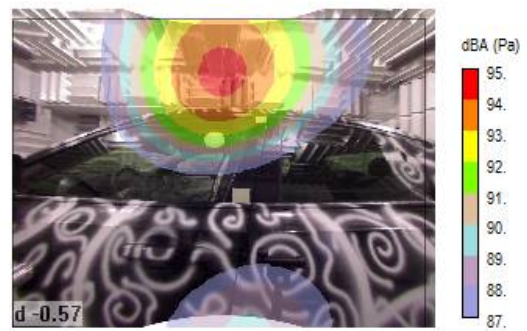
(a) Car 1: 600 - 680 Hz



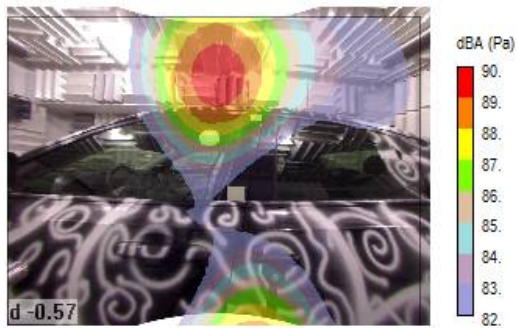
(b) Car 1: 720 - 880 Hz



(c) Car 1: 920 - 1120 Hz



(d) Car 1: 1160 - 1400 Hz



(e) Car 1: 1440 - 1760 Hz



(f) Car 1: 1800 - 2240 Hz

Figure A.4.: Position: Striker



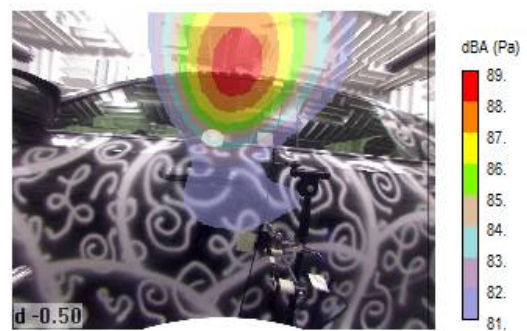
(a) Car 1: 600 - 680 Hz



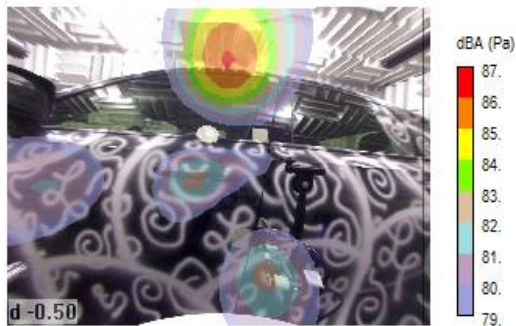
(b) Car 1: 720 - 880 Hz



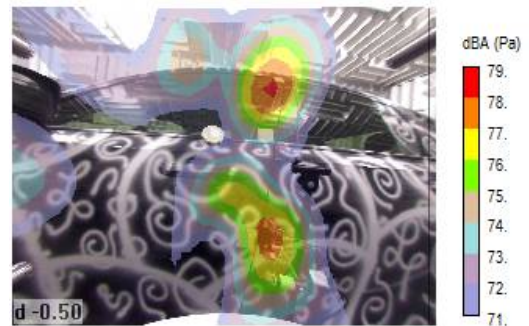
(c) Car 1: 920 - 1120 Hz



(d) Car 1: 1160 - 1400 Hz



(e) Car 1: 1440 - 1760 Hz



(f) Car 1: 1800 - 2240 Hz

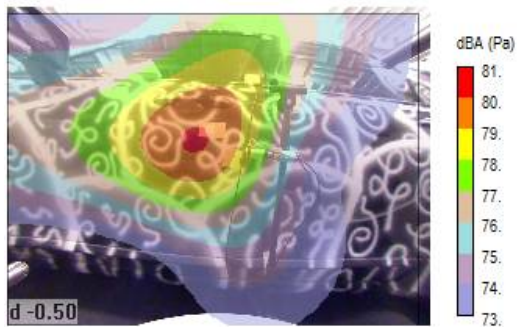
Figure A.5.: Position: Lower Rail Right



(a) Car 1: 600 - 680 Hz



(b) Car 1: 720 - 880 Hz



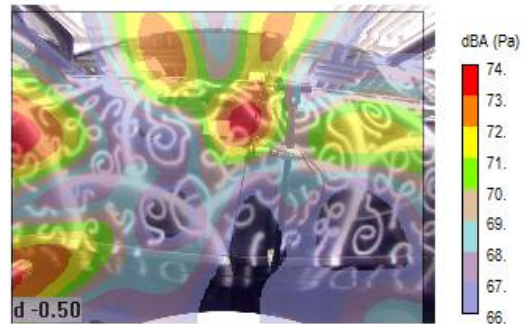
(c) Car 1: 920 - 1120 Hz



(d) Car 1: 1160 - 1400 Hz



(e) Car 1: 1440 - 1760 Hz



(f) Car 1: 1800 - 2240 Hz

Figure A.6.: Position: Lower Rail



(a) Car 1: 600 - 680 Hz



(b) Car 1: 720 - 880 Hz



(c) Car 1: 920 - 1120 Hz



(d) Car 1: 1160 - 1400 Hz



(e) Car 1: 1440 - 1760 Hz



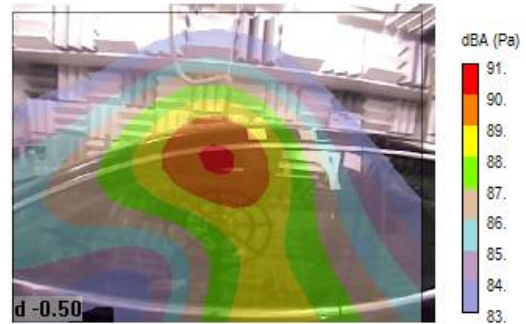
(f) Car 1: 1800 - 2240 Hz

## A.2. Car 2

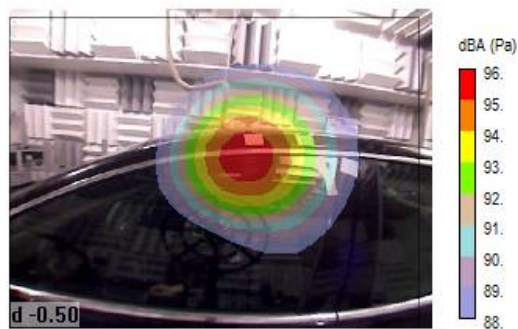
Figure A.7.: Position: Upper Rail Right



(a) Car 2: 600 - 680 Hz



(b) Car 2: 720 - 880 Hz



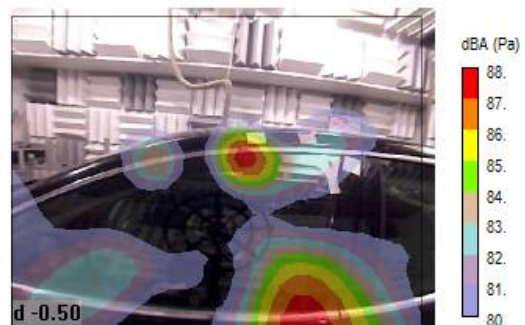
(c) Car 2: 920 - 1120 Hz



(d) Car 2: 1160 - 1400 Hz

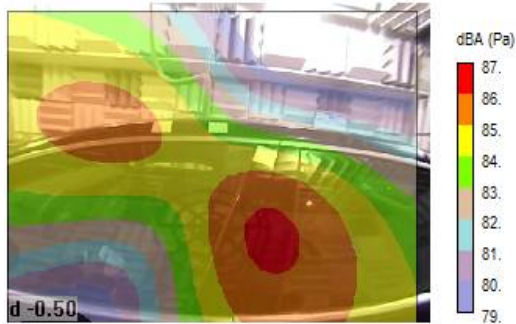


(e) Car 2: 1440 - 1760 Hz

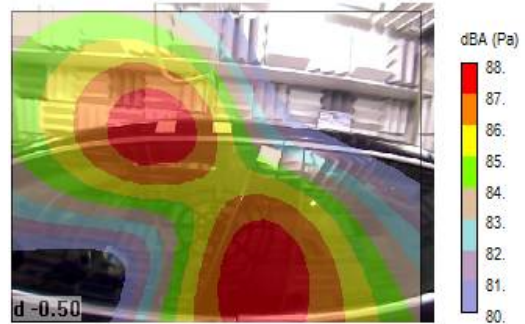


(f) Car 2: 1800 - 2240 Hz

Figure A.8.: Position: Frame Top



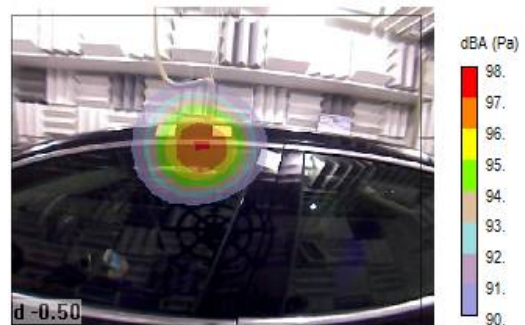
(a) Car 2: 600 - 680 Hz



(b) Car 2: 720 - 880 Hz



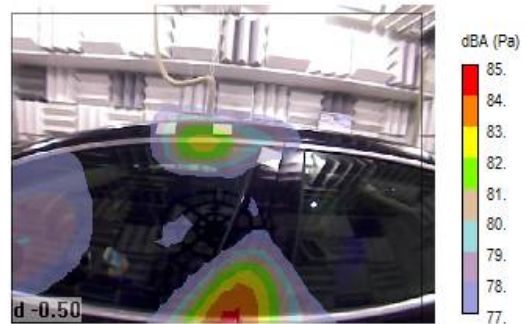
(c) Car 2: 920 - 1120 Hz



(d) Car 2: 1160 - 1400 Hz

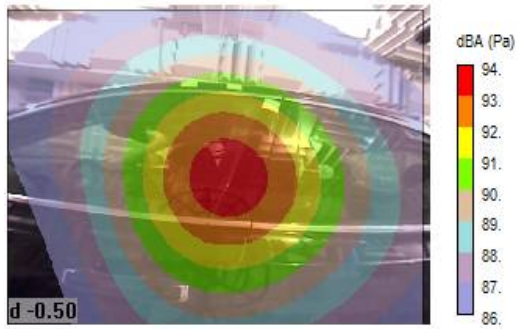


(e) Car 2: 1440 - 1760 Hz

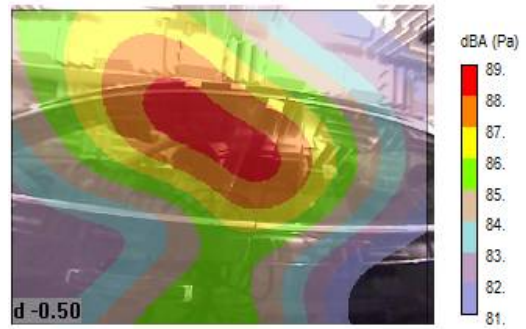


(f) Car 2: 1800 - 2240 Hz

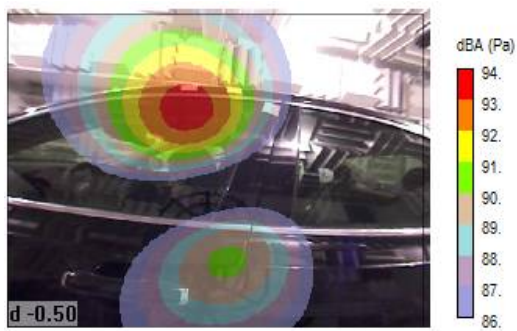
Figure A.9.: Position: Frame Bottom



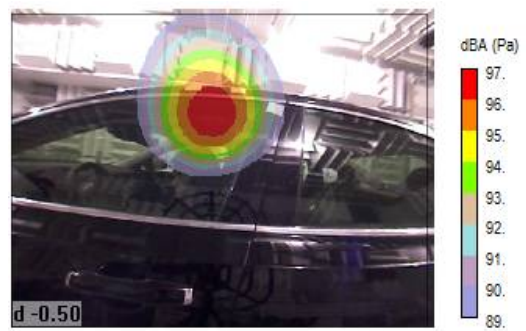
(a) Car 2: 600 - 680 Hz



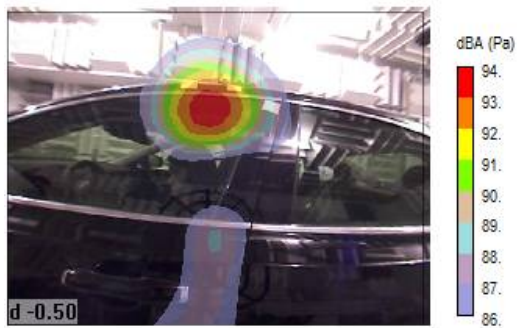
(b) Car 2: 720 - 880 Hz



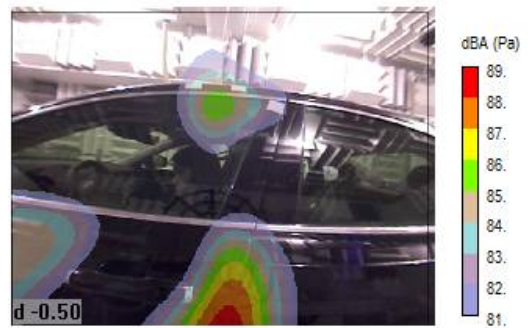
(c) Car 2: 920 - 1120 Hz



(d) Car 2: 1160 - 1400 Hz

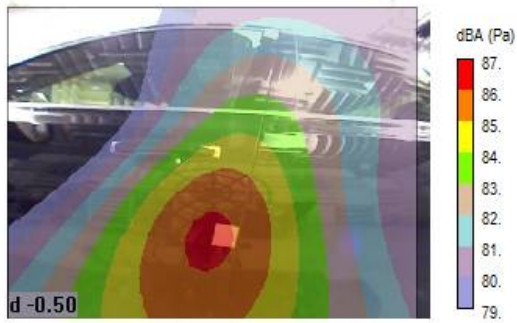


(e) Car 2: 1440 - 1760 Hz

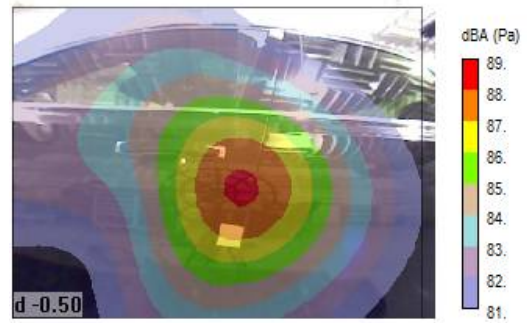


(f) Car 2: 1800 - 2240 Hz

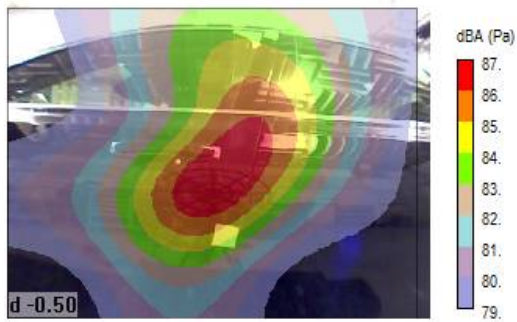
Figure A.10.: Position: Striker



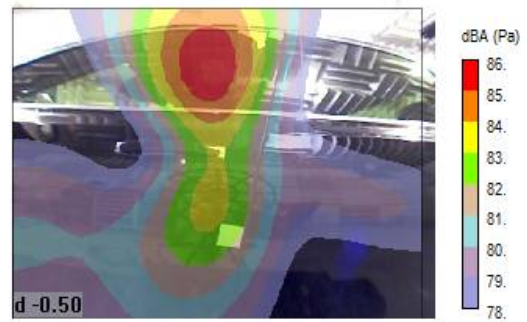
(a) Car 2: 600 - 680 Hz



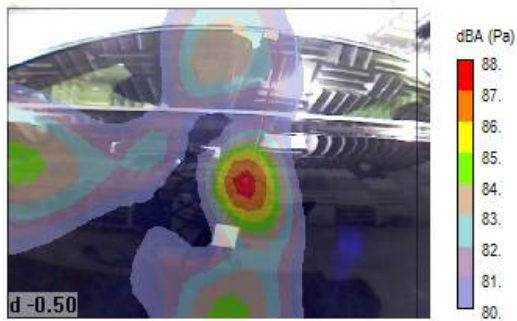
(b) Car 2: 720 - 880 Hz



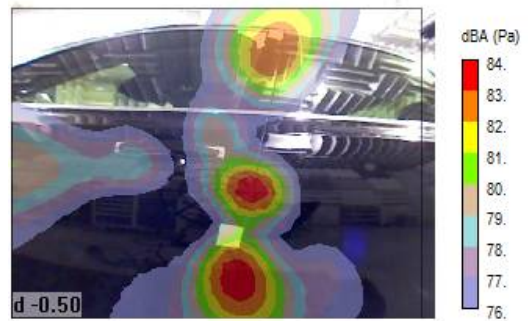
(c) Car 2: 920 - 1120 Hz



(d) Car 2: 1160 - 1400 Hz



(e) Car 2: 1440 - 1760 Hz

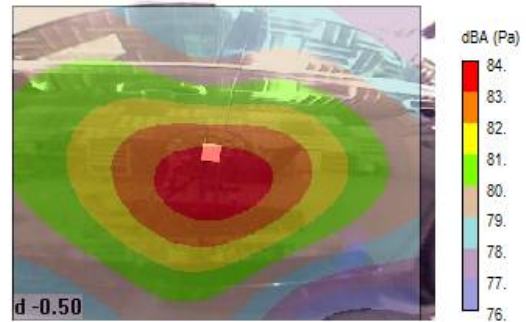


(f) Car 2: 1800 - 2240 Hz

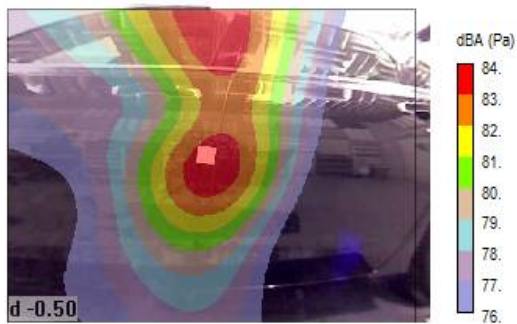
Figure A.11.: Position: Lower Rail Right



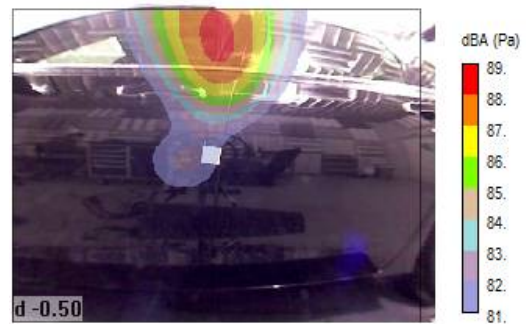
(a) Car 2: 600 - 680 Hz



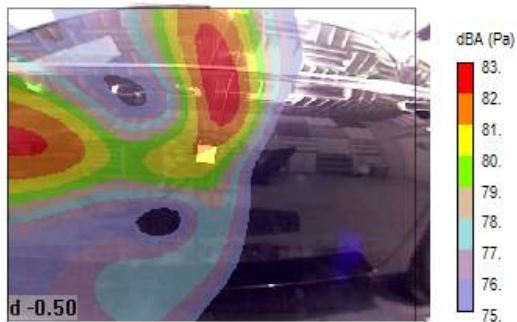
(b) Car 2: 720 - 880 Hz



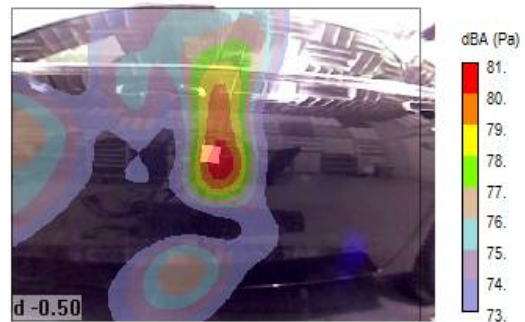
(c) Car 2: 920 - 1120 Hz



(d) Car 2: 1160 - 1400 Hz



(e) Car 2: 1440 - 1760 Hz



(f) Car 2: 1800 - 2240 Hz

## B. Accelerometer and Acoustic Head Measurements

### B.1. Variation of the Layers

The main results of the measurements of varying the stiffness layers are presented here.

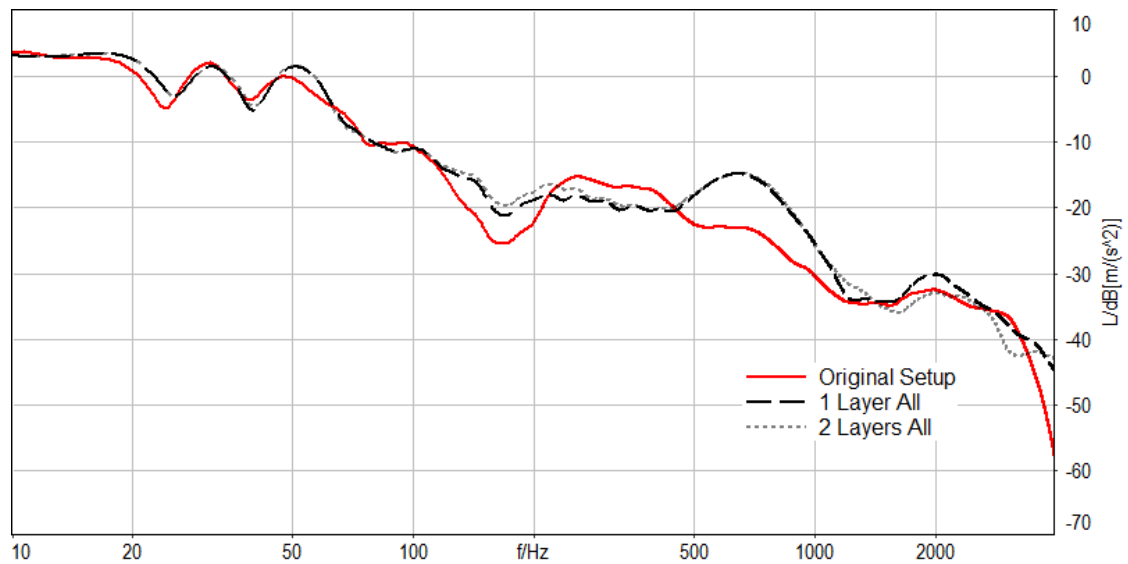


Figure B.1.: Comparison of the accelerometer levels of the original setup and the stiffness variations. Position: Frame Top

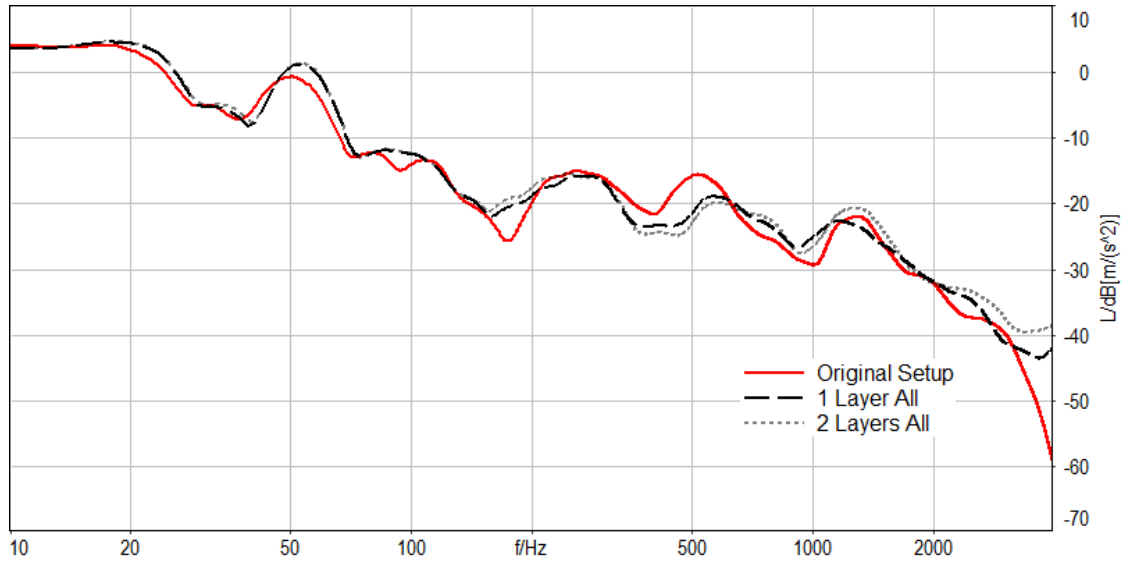


Figure B.2.: Comparison of the accelerometer levels of the original setup and the stiffness variations. Position: Frame Bottom

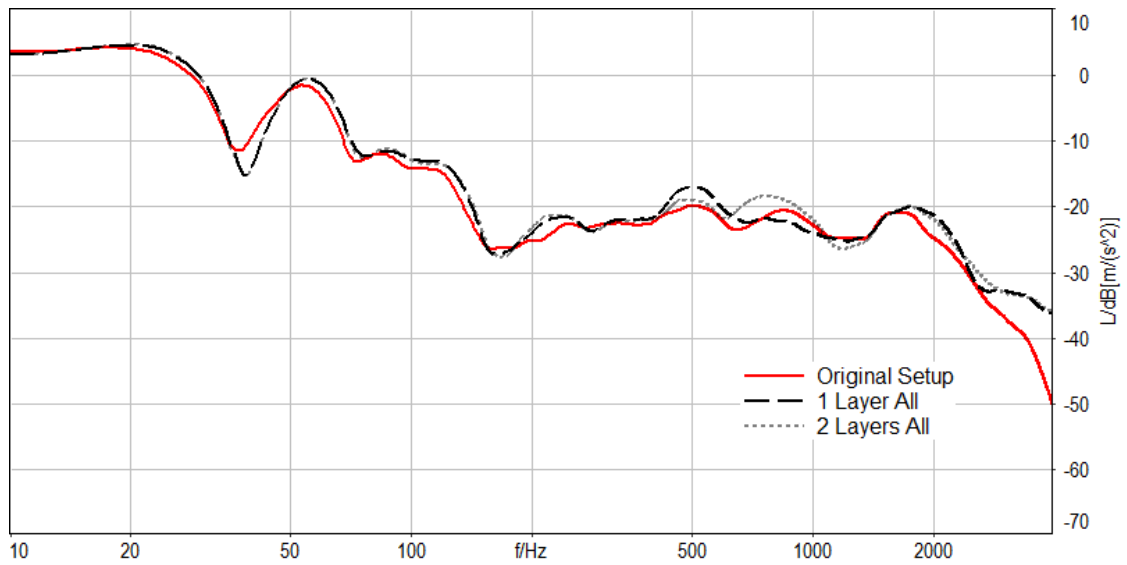


Figure B.3.: Comparison of the accelerometer levels of the original setup and the stiffness variations. Position: Striker

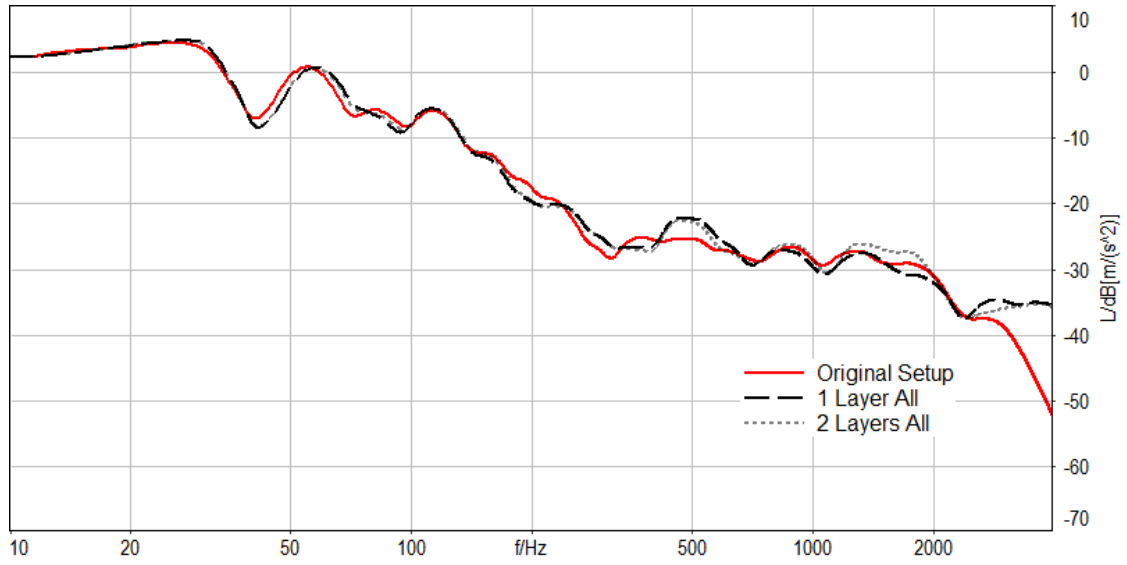


Figure B.4.: Comparison of the accelerometer levels of the original setup and the stiffness variations. Position: Lower Rail Right

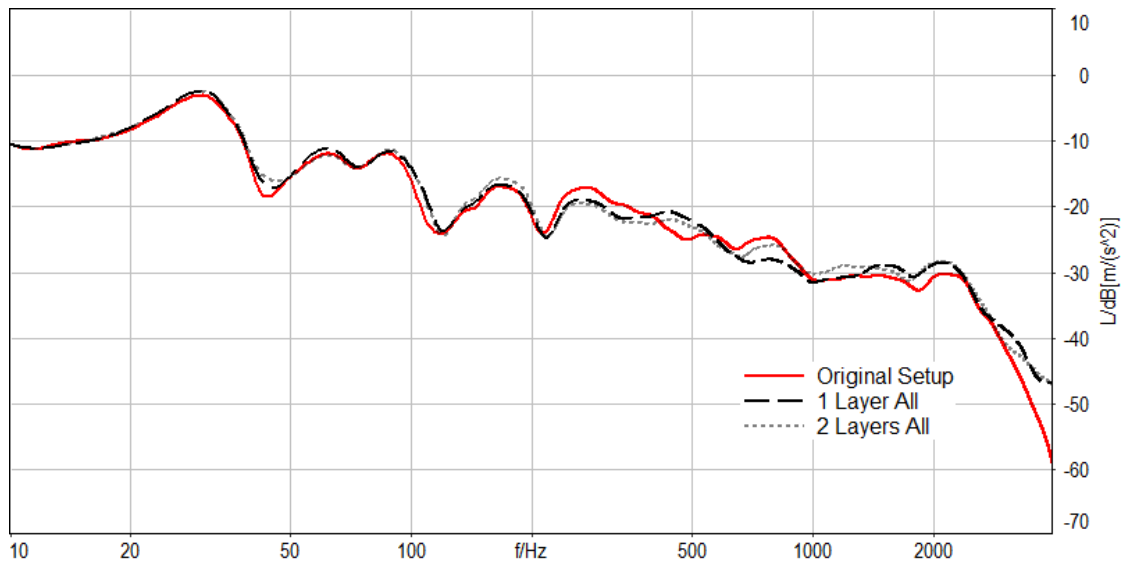


Figure B.5.: Comparison of the accelerometer levels of the original setup and the stiffness variations. Position: Lower Rail Left

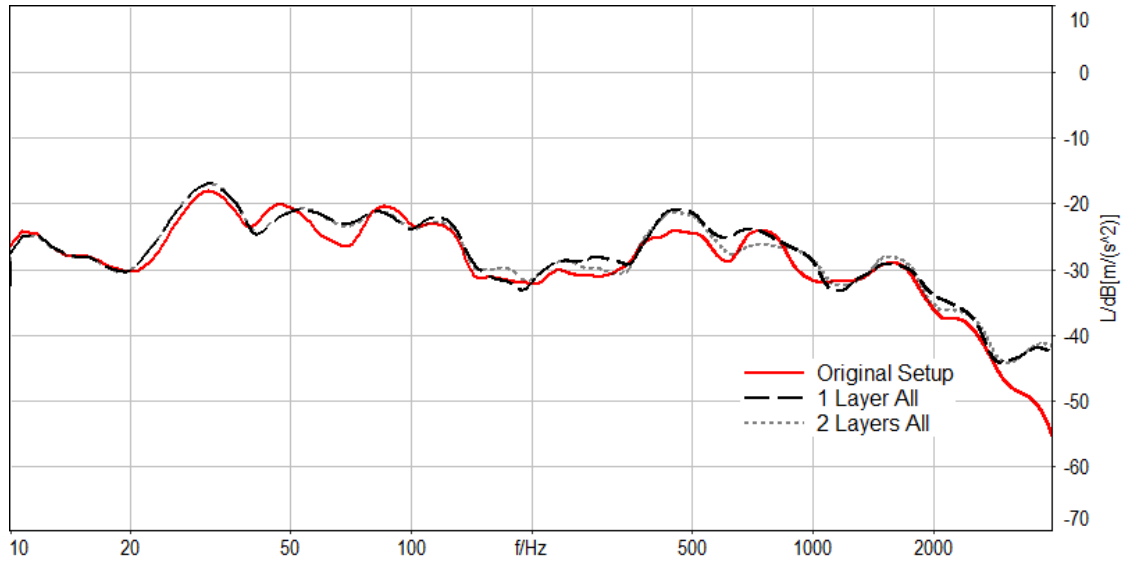


Figure B.6.: Comparison of the accelerometer levels of the original setup and the stiffness variations. Position: A Pillar

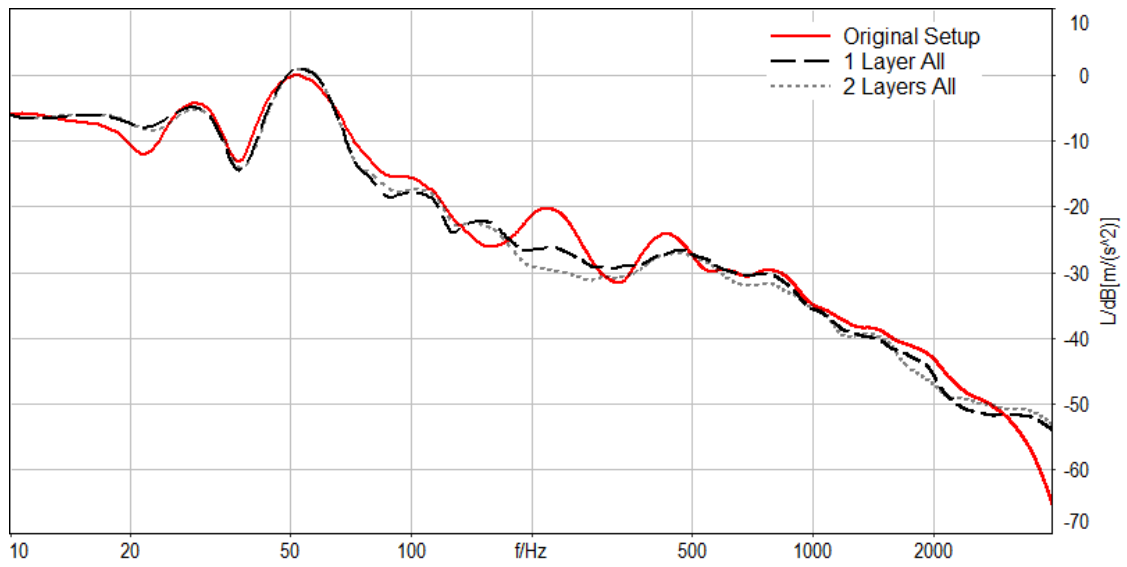


Figure B.7.: Comparison of the accelerometer levels of the original setup and the stiffness variations. Position: Upper Rail Left

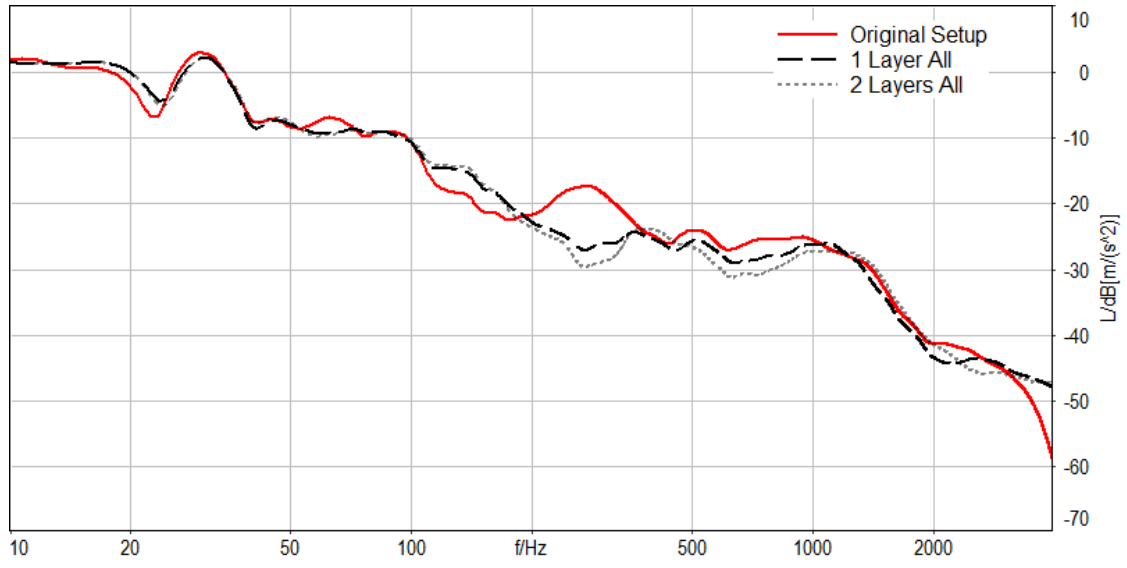


Figure B.8.: Comparison of the accelerometer levels of the original setup and the stiffness variations. Position: Upper Rail Right

## B.2. Single Stiffness Variations

The main results of the measurements of varying the stiffness layers are presented here.

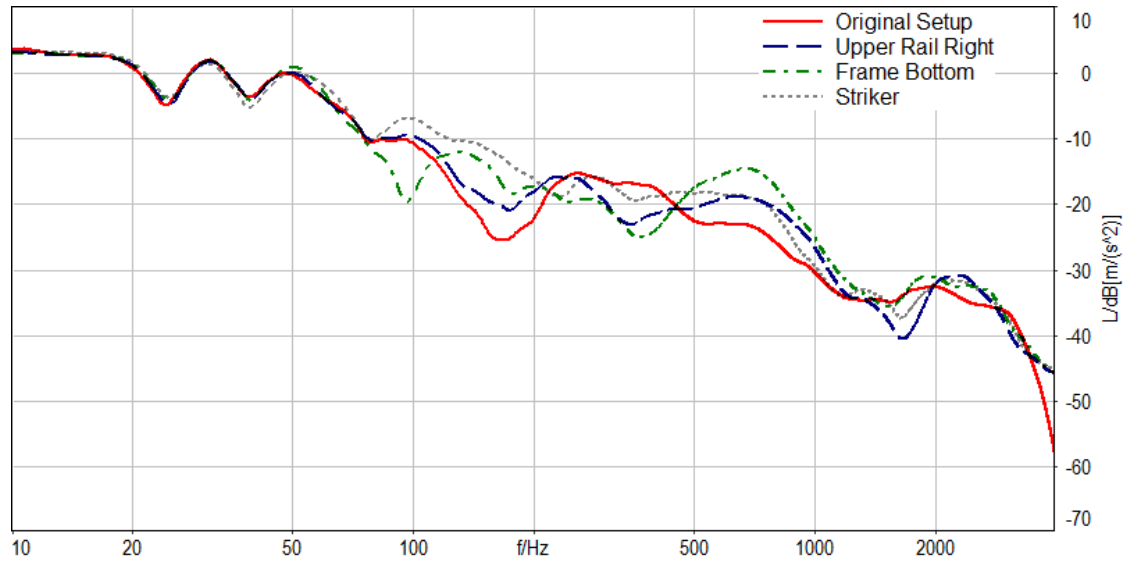


Figure B.9.: Comparison of the accelerometer levels of the original setup and the stiffness variations. Position: Frame Top

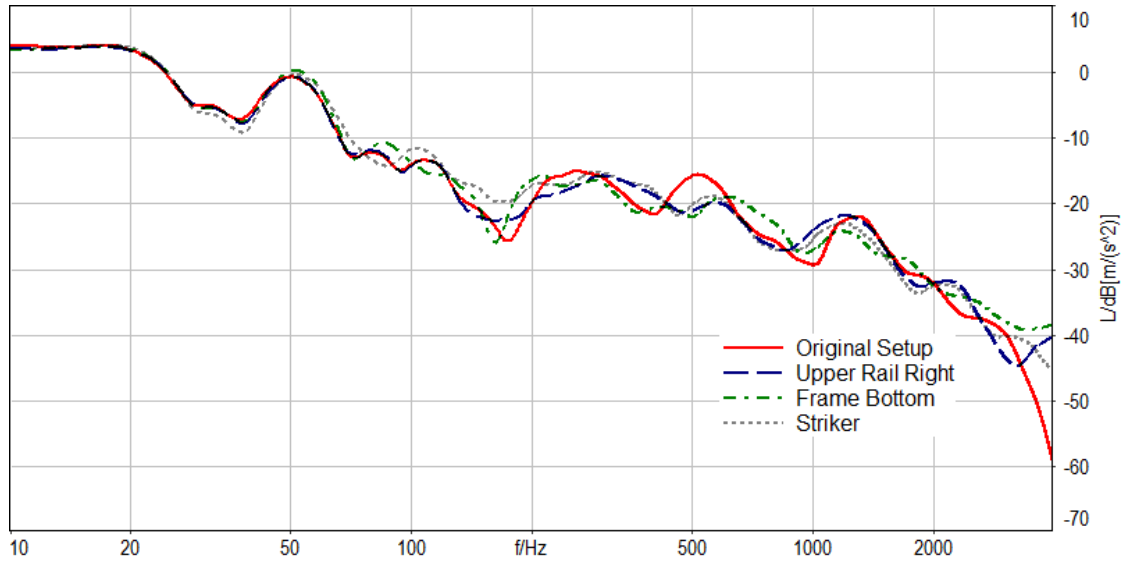


Figure B.10.: Comparison of the accelerometer levels of the original setup and the stiffness variations. Position: Frame Bottom

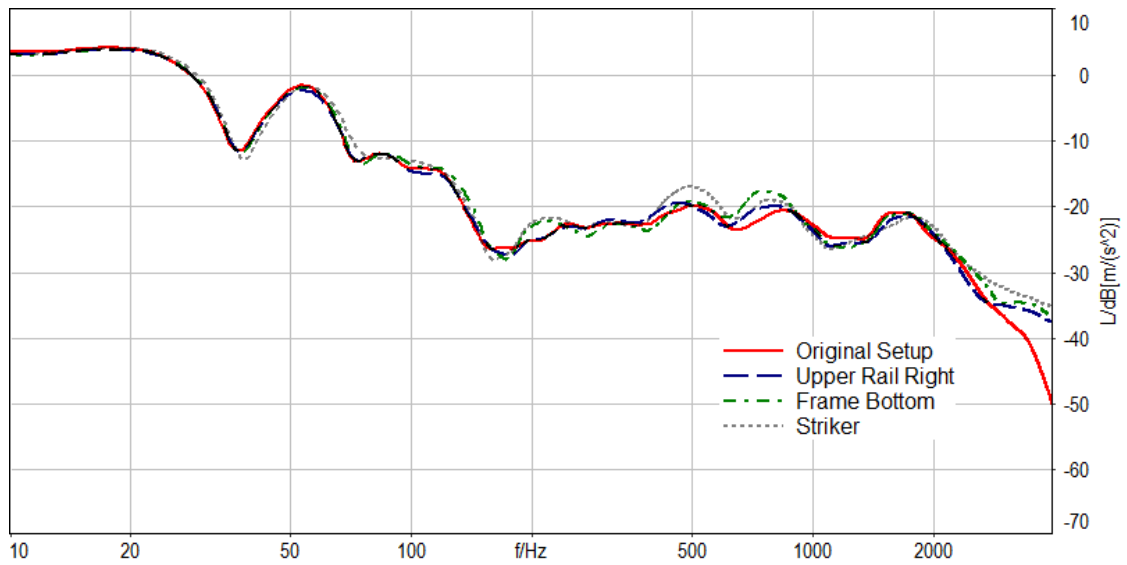


Figure B.11.: Comparison of the accelerometer levels of the original setup and the stiffness variations. Position: Striker

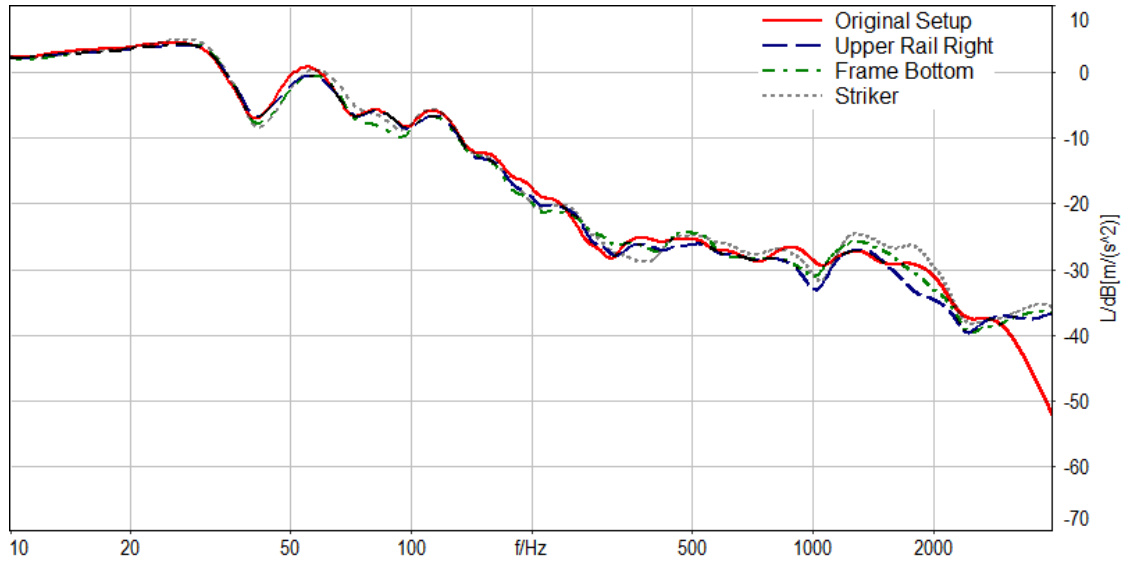


Figure B.12.: Comparison of the accelerometer levels of the original setup and the stiffness variations. Position: Lower Rail Right

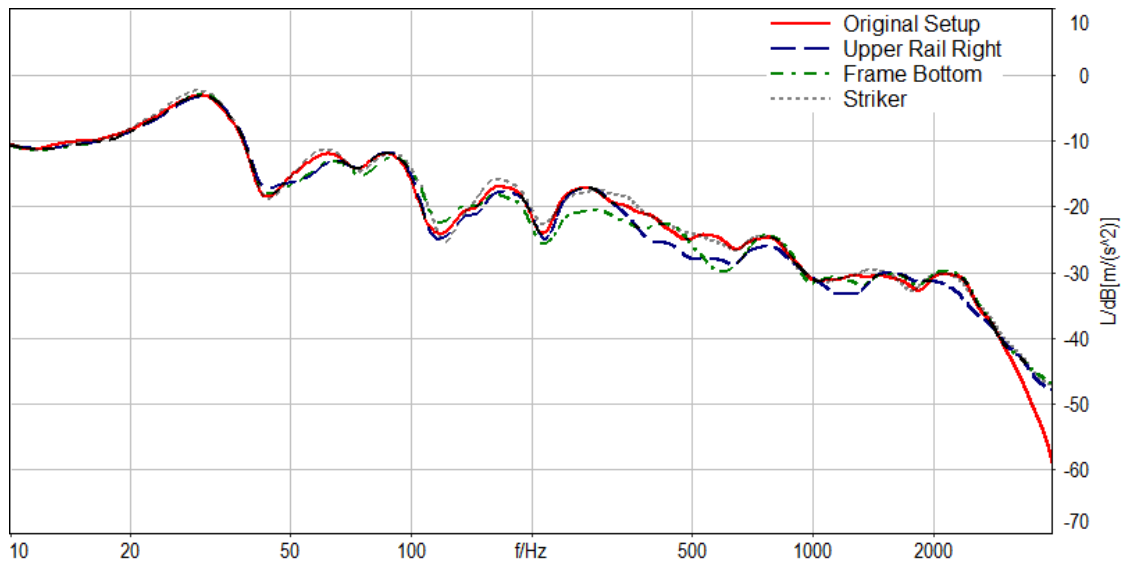


Figure B.13.: Comparison of the accelerometer levels of the original setup and the stiffness variations. Position: Lower Rail Left

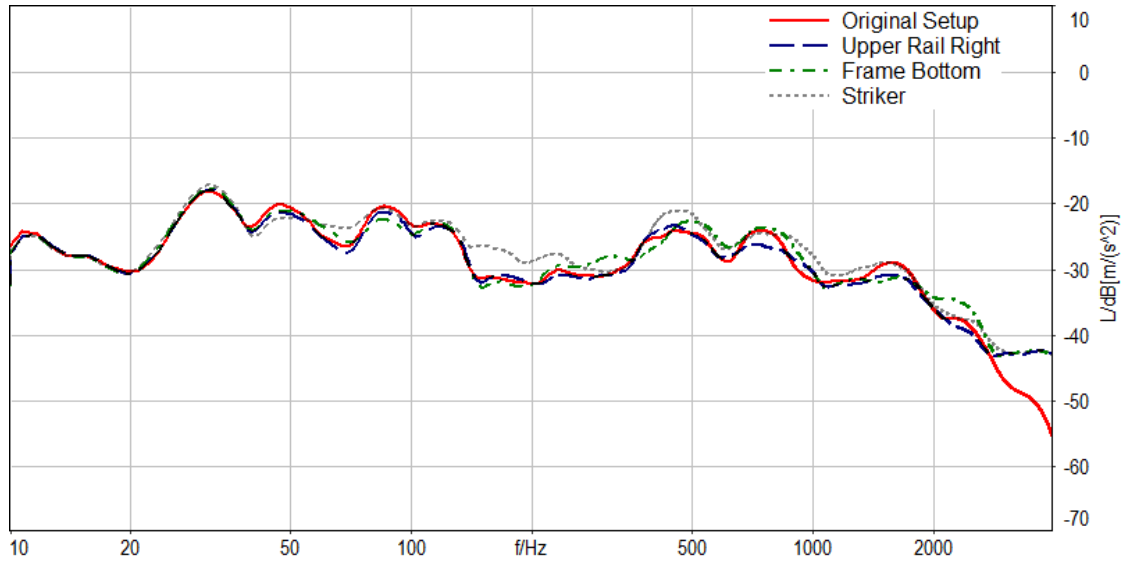


Figure B.14.: Comparison of the accelerometer levels of the original setup and the stiffness variations. Position: A Pillar

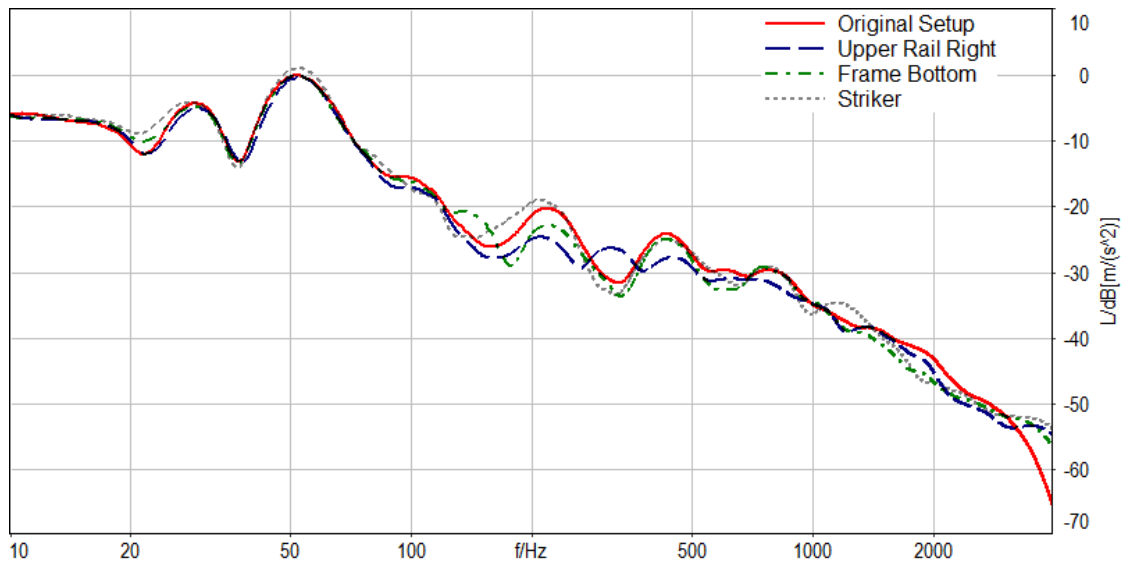


Figure B.15.: Comparison of the accelerometer levels of the original setup and the stiffness variations. Position: Upper Rail Left

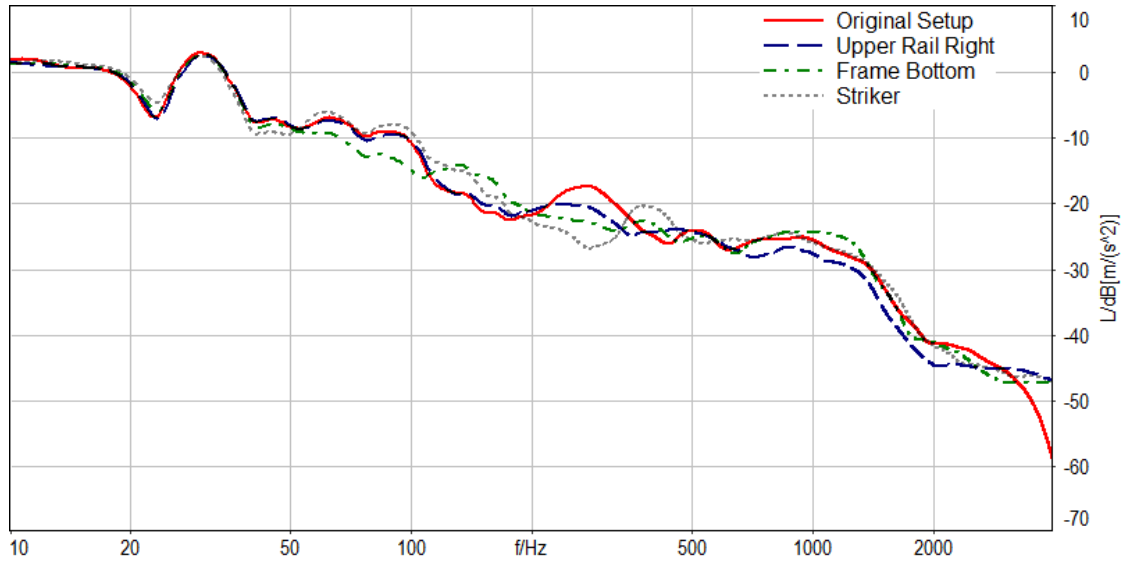


Figure B.16.: Comparison of the accelerometer levels of the original setup and the stiffness variations. Position: Upper Rail Right

### B.3. Front Versus Back Inclination

The main results of the measurements of varying the inclination from the left and right are presented here.

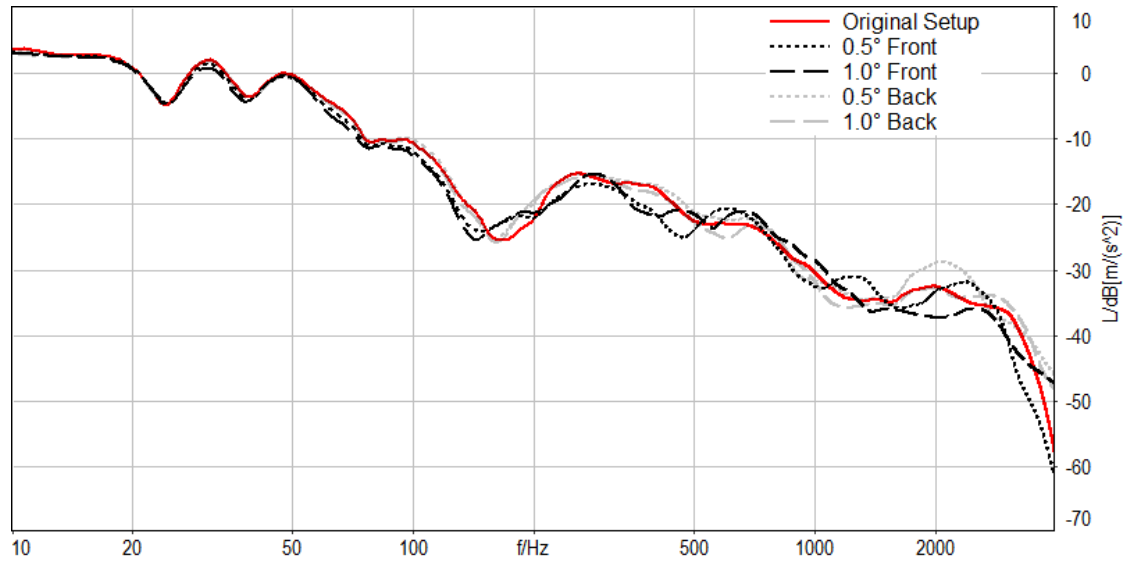


Figure B.17.: Comparison of the accelerometer levels of the original setup and the inclination (front versus back) variations. Position: Frame Top

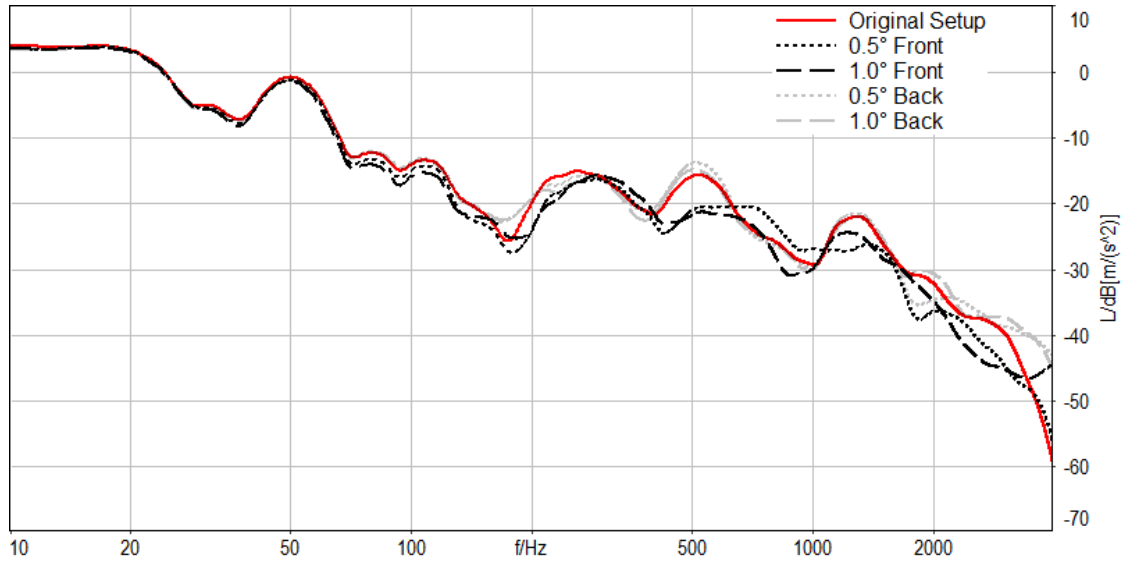


Figure B.18.: Comparison of the accelerometer levels of the original setup and the inclination (front versus back) variations. Position: Frame Bottom

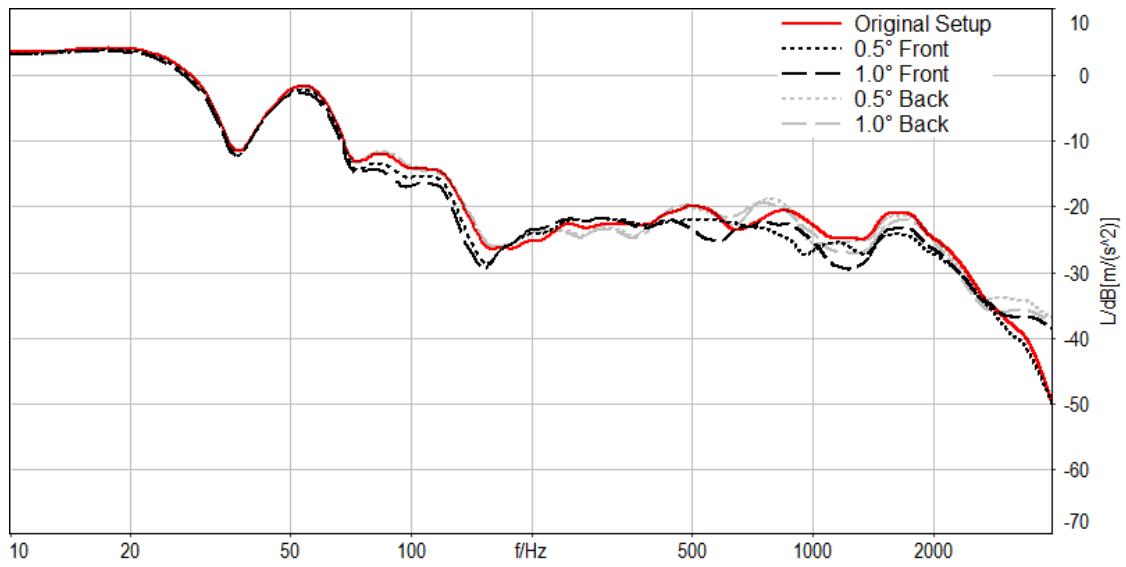


Figure B.19.: Comparison of the accelerometer levels of the original setup and the inclination (front versus back) variations. Position: Striker

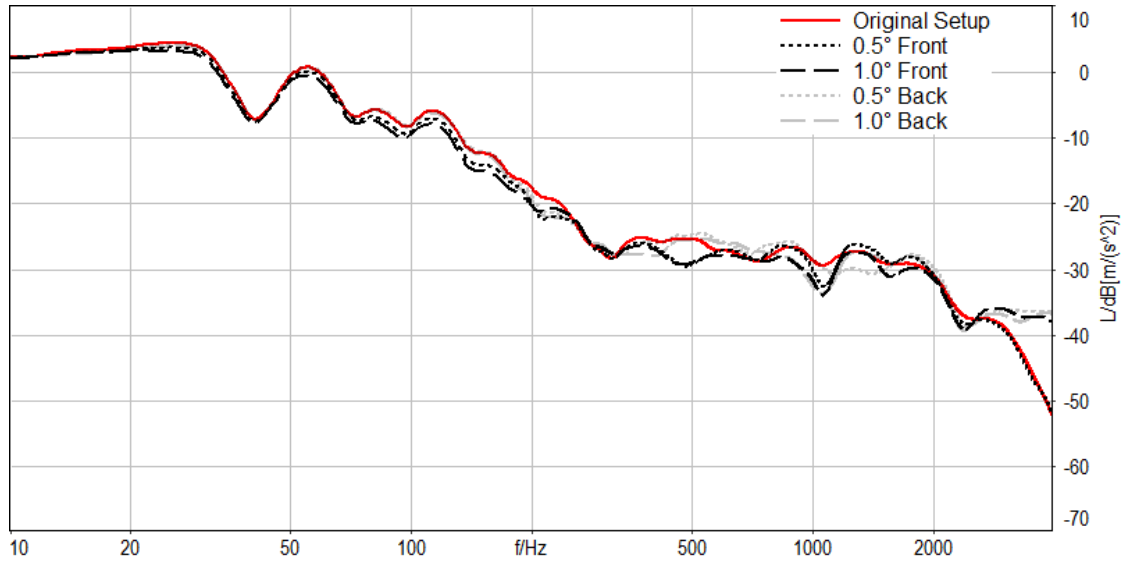


Figure B.20.: Comparison of the accelerometer levels of the original setup and the inclination (front versus back) variations. Position: Lower Rail Right

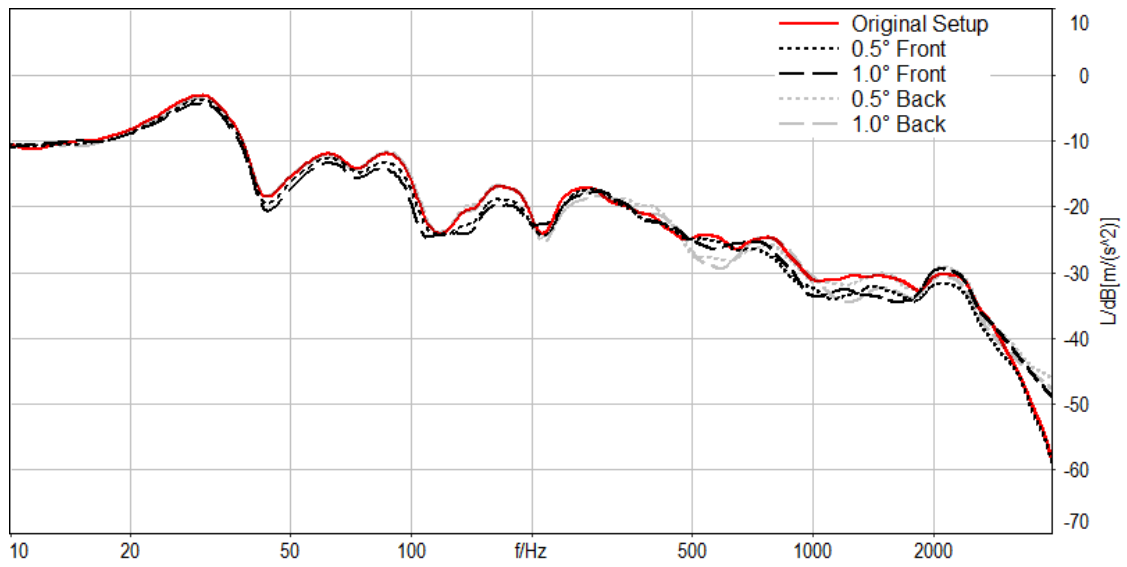


Figure B.21.: Comparison of the accelerometer levels of the original setup and the inclination (front versus back) variations. Position: Lower Rail Left

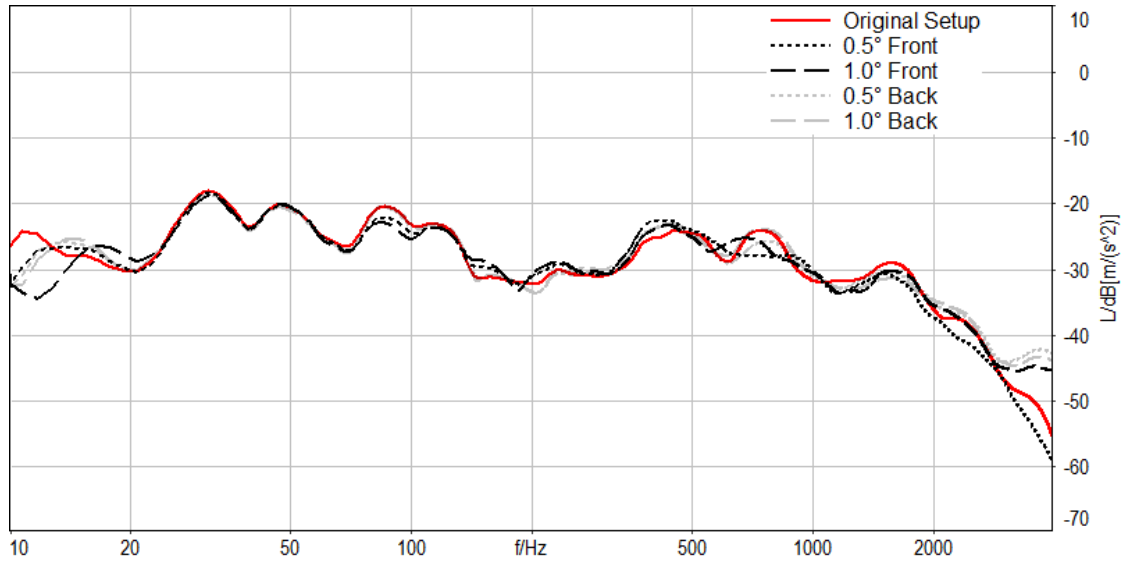


Figure B.22.: Comparison of the accelerometer levels of the original setup and the inclination (front versus back) variations. Position: A Pillar

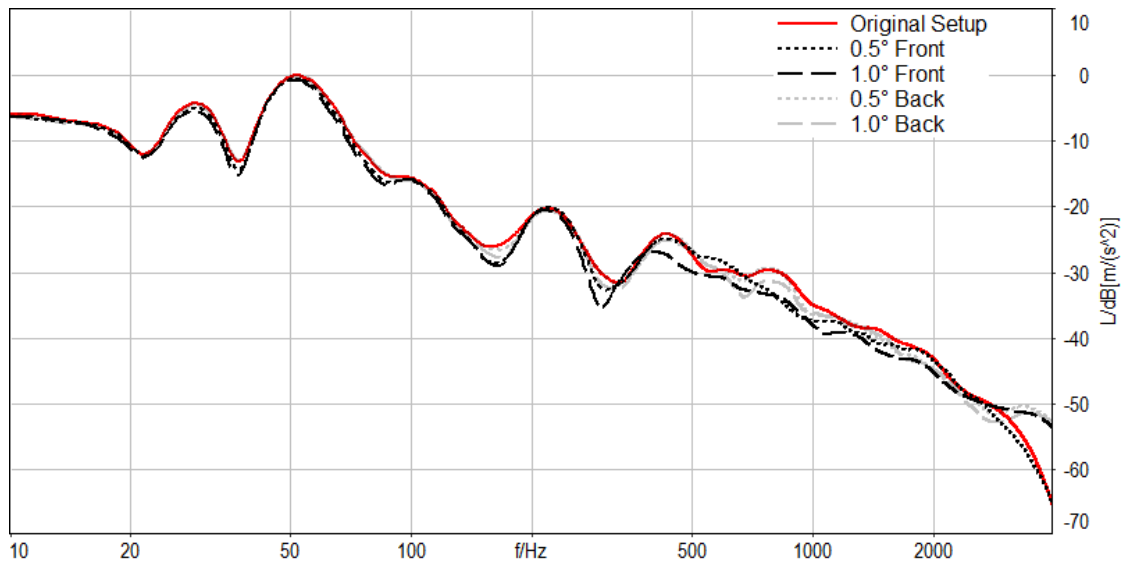


Figure B.23.: Comparison of the accelerometer levels of the original setup and the inclination (front versus back) variations. Position: Upper Rail Left

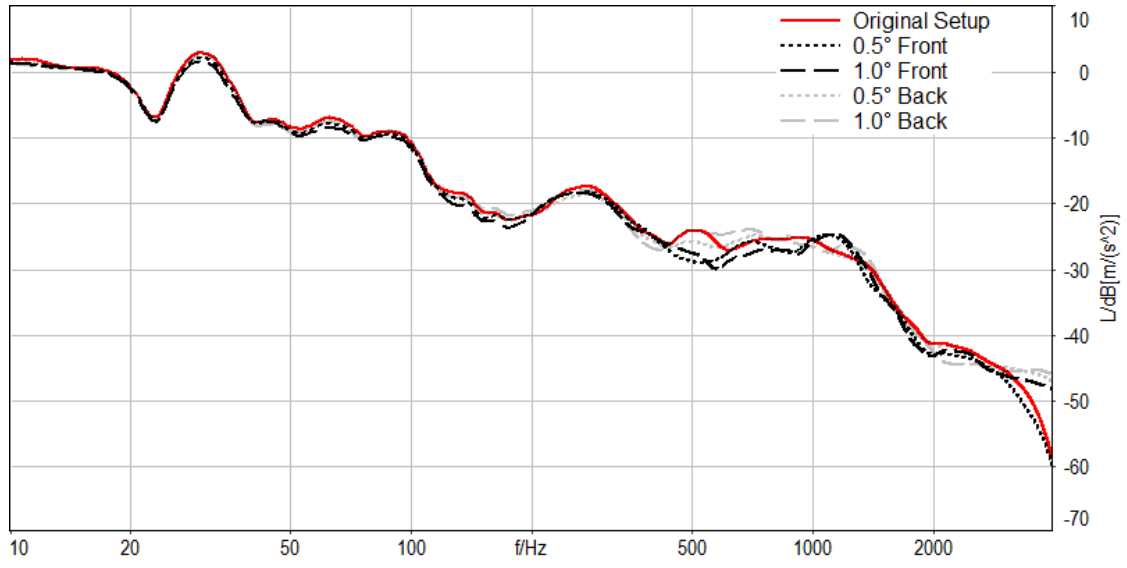


Figure B.24.: Comparison of the accelerometer levels of the original setup and the inclination (front versus back) variations. Position: Upper Rail Right

## B.4. Left versus Right Inclination

The main results of the measurements of varying the inclination from the left and right are presented here.

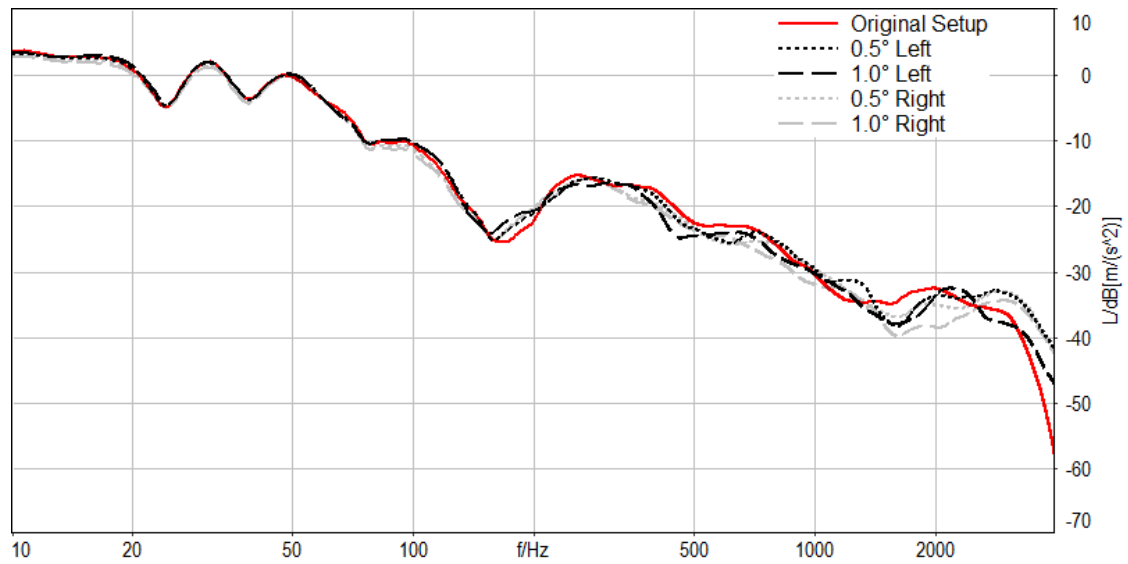


Figure B.25.: Comparison of the accelerometer levels of the original setup and the inclination (left versus right) variations. Position: Frame Top

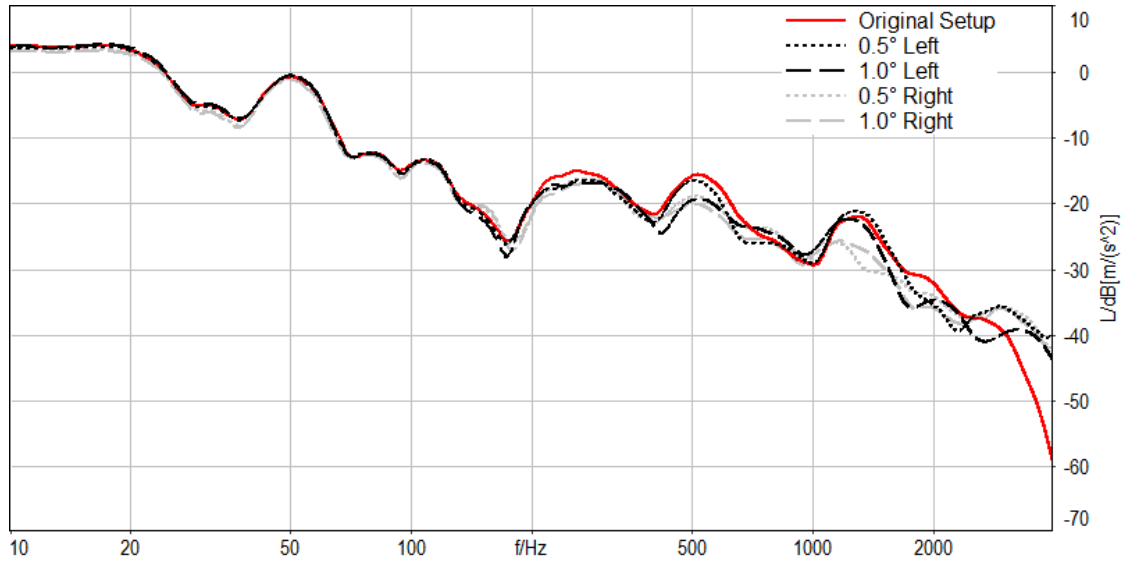


Figure B.26.: Comparison of the accelerometer levels of the original setup and the inclination (left versus right) variations. Position: Frame Bottom

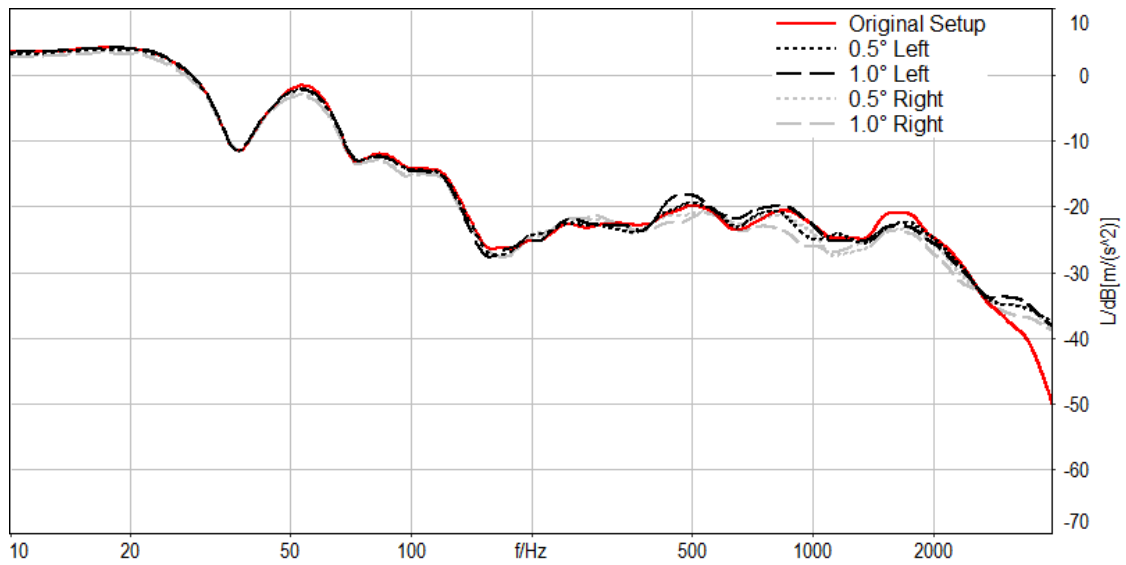


Figure B.27.: Comparison of the accelerometer levels of the original setup and the inclination (left versus right) variations. Position: Striker

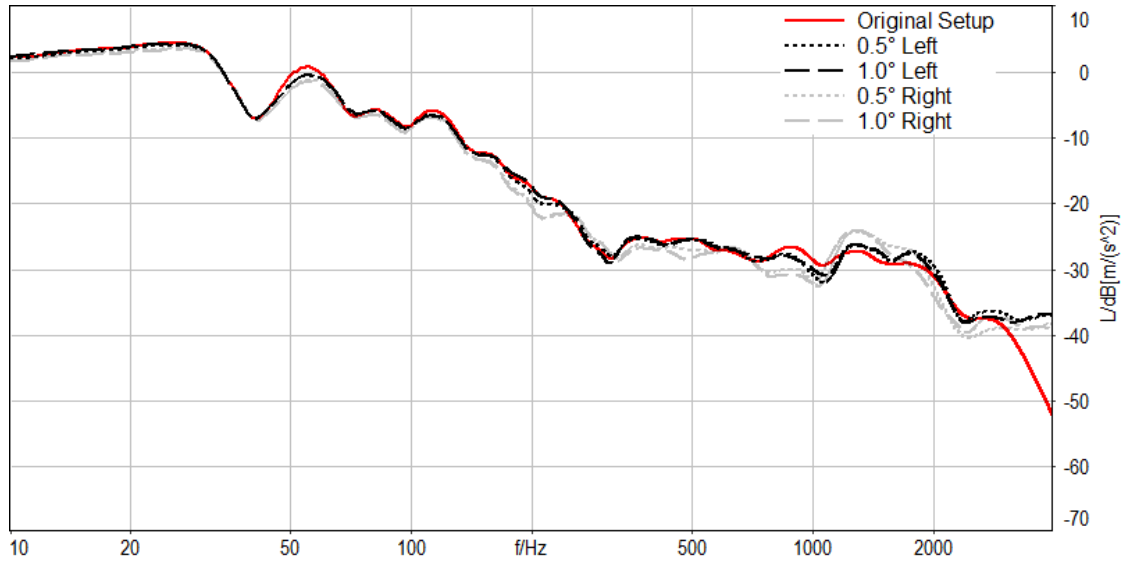


Figure B.28.: Comparison of the accelerometer levels of the original setup and the inclination (left versus right) variations. Position: Lower Rail Right

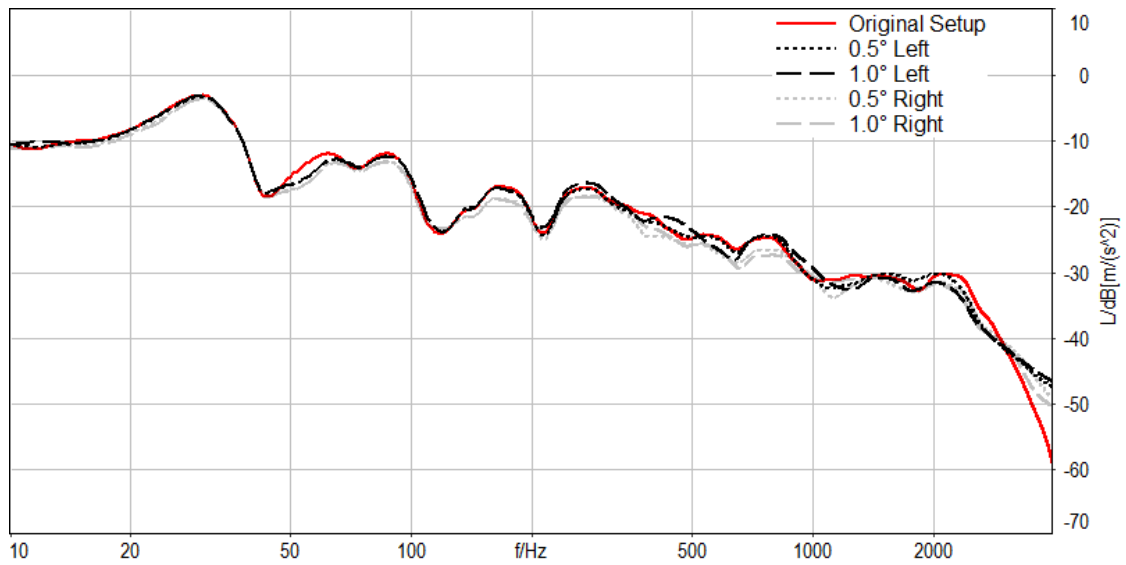


Figure B.29.: Comparison of the accelerometer levels of the original setup and the inclination (left versus right) variations. Position: Lower Rail Left

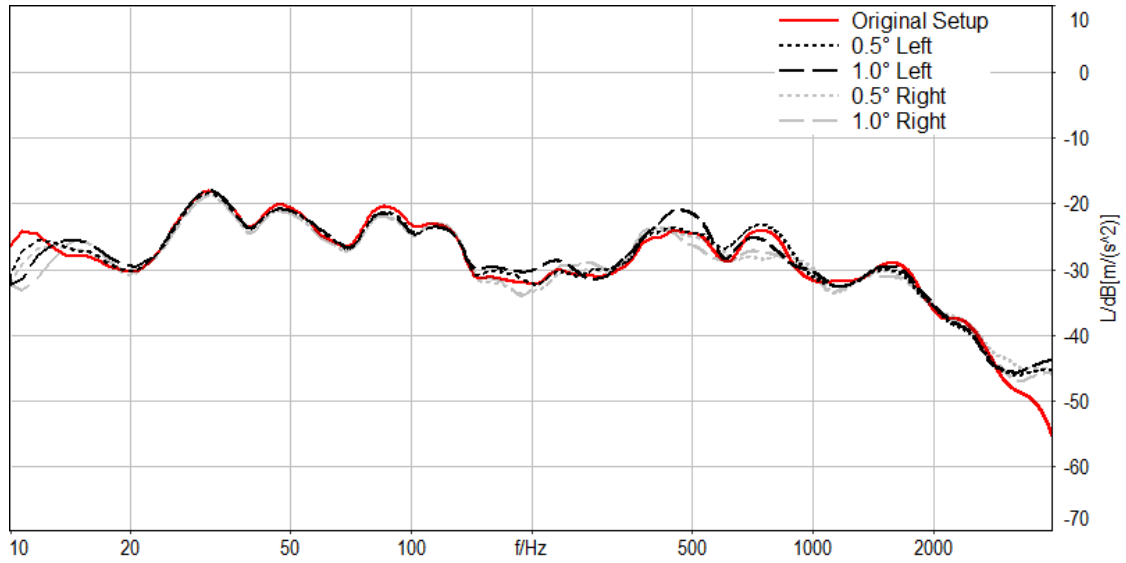


Figure B.30.: Comparison of the accelerometer levels of the original setup and the inclination (left versus right) variations. Position: A Pillar

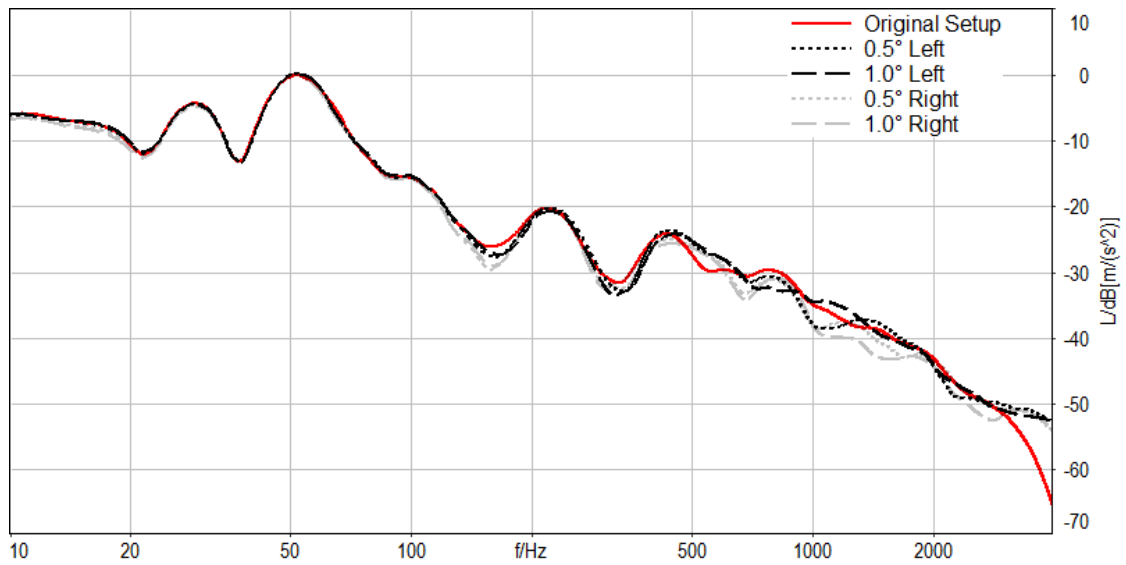


Figure B.31.: Comparison of the accelerometer levels of the original setup and the inclination (left versus right) variations. Position: Upper Rail Left

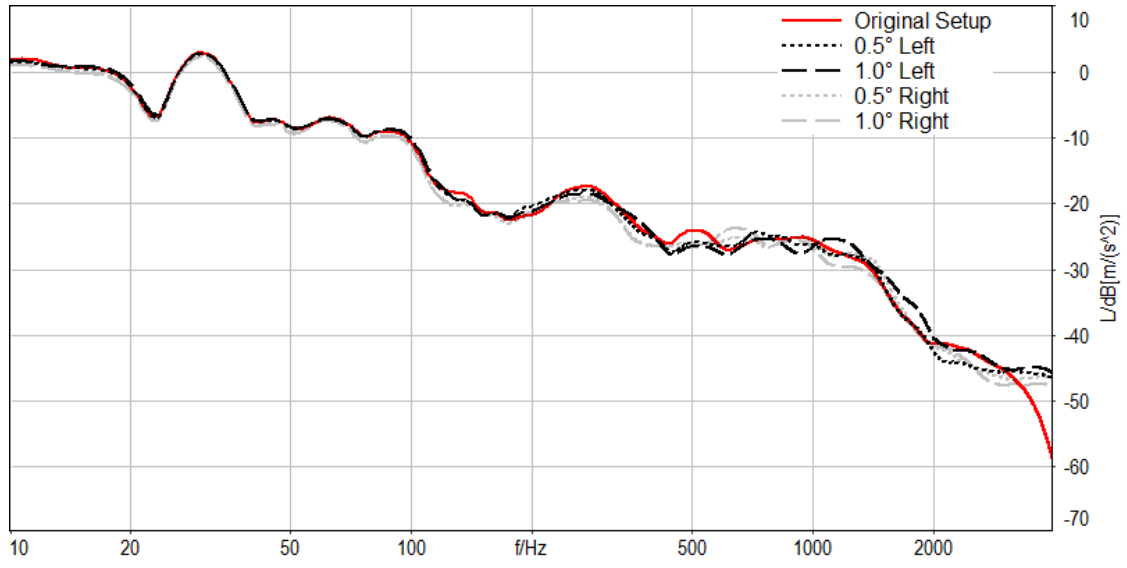


Figure B.32.: Comparison of the accelerometer levels of the original setup and the inclination (left versus right) variations. Position: Upper Rail Right